THE USE OF RAPID PRESSURE SWING ADSORPTION TO ENHANCE THE DESIGN OF PORTABLE MEDICAL OXYGEN CONCENTRATORS

A Thesis Submitted for the Degree of Master of Philosophy

By

Callum Kenny

Chemical Engineering, Brunel University London

31st July 2024

ABSTRACT

Portable oxygen concentrators are restricted by three main factors: power consumption, weight and output. To minimise the weight and output of a portable oxygen concentrator. This paper investigates how rapid pressure swing adsorption will improve oxygen yield per unit volume of adsorbent. It was observed through experimental data the rapid pressure swing adsorption cycle developed in this research could achieve a throughput of 50 sccm, using adsorbent Zeox Z12-49, in one 6.4mm diameter column of 140mm in length, which is a four times improvement when compared to leading market devices.

TABLE OF CONTENTS

LIST OF TABLES

LIST OF FIGURES

ACRONYMS

Table 1: Table of Acronyms

Acronym	Description
COPD	Chronic Obstructive Pulmonary Disease
LPM	Litres per minute
MTC	Mass Transfer Coefficient
MTZ	Mass Transfer Zone
POC	Portable Oxygen Concentrator
PPSA	Pulsed Pressure Swing Adsorption
PSA	Pressure Swing Adsorption
RPSA	Rapid Pressure Swing Adsorption
TSA	Thermal Swing Adsorption
URPSA	Ultra Rapid Pressure Swing Adsorption
VPSA	Vacuum Pressure Swing Adsorption
WHO	World Health Organisation

DEFINITIONS

Table 2: Table of Definitions

Abbreviation	Definition
r_p	Adsorbent particle radius
D_L	Axial Dispersion
ε_b	Bed voidage
K_p	Constant that measures permeability of the porous media
k_i	Dispersive resistances
z	Distance measured from column inlet
k_f	External fluid film mass transfer coefficient
η	Fluid velocity
K	Henry's law constant
v_z	Interstitial velocity
D_{ci}	Intracrystalline diffusivity
γ_2	Inverse of the limiting Peclet number
L	Length
Pe_∞	Limiting Peclet number
r_c	Microparticle radius
D_m	Molecular diffusivity
d_p	Particle diameter
Pe	Peclet number
D_{pi}	Pore Diffusivity
ε_p	Porosity of adsorbent particle

Table 2: Table of Definitions (Continued)

Abbreviation	Definition
Δp	Pressure drop
β	Radial dispersion factor
Re	Reynolds number
c_i/ n_i	Sorbate concentration (of component i) in fluid phase
u_z	Superficial velocity
t	Time
ρ	Total fluid density
γ_1	Touristy factor

1. INTRODUCTION

Three of the top 10 global causes of death, as listed by the World Health Organisation (WHO), are respiratory based. Chronic Obstructive Pulmonary Diseases (COPD) being the highest, claiming 6% of all deaths annually worldwide (Chronic Respiratory Diseases n.d.). This does not take into consideration the 2019 novel coronavirus (COVID-19) which is also a respiratory infection that, at the time of writing this report, has claimed more than 1,800,000 lives.

COPD is the term used for a collection of lung conditions, with the diseases falling into two main groups: Bronchitis and Emphysema. Bronchitis is a condition characterised by inflammation of the airways and/or excessive sputum, and Emphysema is a breakdown in the air sacs in the lung(s) (Chronic Obstructive Pulmonary Disease n.d.). Such conditions can result in difficulty breathing, ultimately leading to a drop in blood oxygen levels. At present there is no cure for COPD, but the progression of the disease can be slowed down using oxygen (O_2) therapy and exercise, which can improve those who are sufferings ability to breathe.

COVID-19 is an airborne disease that infects the tracheobronchial tree. Exposure to this disease causes the lining of the airway to become infected and, in turn, the lungs begin to generate an inflammatory material. When the lungs fill with this inflammatory material, they are unable to deliver enough O_2 into the bloodstream which reduces the suffers blood O_2 saturation levels. Even after recovery from COVID-19, there can be long-lasting damage to the lungs which continues to limit the volume of O_2 which can be adsorbed by the lungs. Due to this, O_2 therapy has been critical in treating COVID-19 patients in both the hospital and at home environments.

The incumbent method for O_2 therapy when away from the hospital environment is using a high-pressure O_2 cylinder (Chronic Obstructive Pulmonary Disease n.d.). This comes with some disadvantages, namely the unportable nature of the heavy cylinders, the duration of use is unclear, they require replacement when empty which makes them expensive, and there are potential hazards involved when handling them due to the high pressures involved (Home Oxygen Therapy n.d.).

An alternative, and much safer option, is to use an O_2 concentrator that purifies air up to 96% O_2. Such devices come in a stationary option that offer the user a high-volume output and an

unlimited supply of O_2. Furthermore, the devices operate at low pressures and, unlike cylinders, there is no refilling required - reducing maintenance and significantly reducing the associated running costs. Whilst stationary devices are ideal in the home environment, they are very large and heavy which does not facilitate ease of transport away from home. Thus, limiting the user's ability to travel away from this environment (Oxygen Concentrator vs. Oxygen Tank Overview n.d.).

A smaller device, known as a Portable Oxygen Concentrator (POC) provides all the same benefits as a stationary oxygen concentrator but in a transportable form. The smaller and lighter weight POC device offers patients the freedom to move away from the home environment and can provide COPD suffers with ambulatory O_2 while they are exercising.

For POC devices to be effective there are three main criteria to consider, see Figure 1. Users need POC devices to be as light weigh as possible so they can exercise; provide the output needed for oxygen therapy; and to have a long battery life to extend exercise (Smallest Portable Oxygen Concentrator: Top Compact Options for On-the-Go Users 27 April 2024).

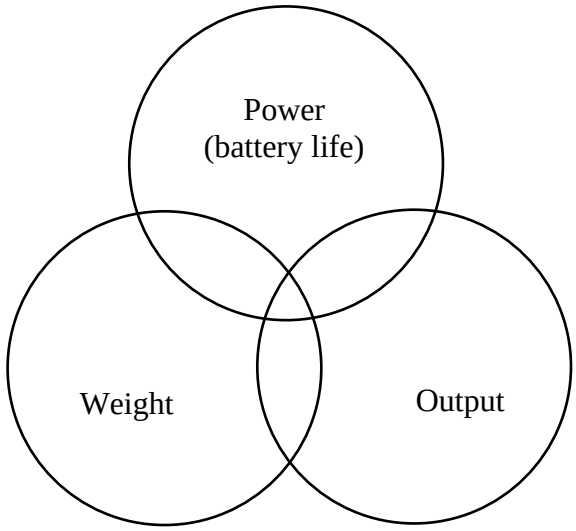

Figure 1: Portable Oxygen Concentrator Venn Diagram

POC devices work by taking atmospheric air and separating it to the main compounds, nitrogen and oxygen, with the oxygen being delivered to the patient. This report will review the available air separation methods, the theory behind air separation, and the oxygen concentrators on the market. Having analysed the accessible data, this report will aim to experimentally develop an air separation method that can improve on one or more of the

attributes; power, weight, and output (Figure 1), to deliver a technological improvement to portable oxygen concentrators that will improve the lives of the users.

2. LITERATURE REVIEW

2.1. Air Separation Processes

The function of a POC is to provide the largest possible volume of high purity O_2 to patients to alleviate lung inefficiencies due to illness whilst remaining as lightweight as possible to be portable and easy to carry.

There are several ways to generate O_2 from air, and they are generally categorised into two methods:

- Cryogenic air separation
- Non-cryogenic air separation
    - Adsorption-based gas separation
    - Membrane based gas separation
    - Chemical processes

Cryogenics is the preferred route for industrial air separation as it is cost effective and highly efficient at producing high purity O_2. The technology is based on low temperature distillation of atmospheric air and the different boiling points of the component gases. Due to the temperatures involved cryogenic separation is not a suitable or safe method to be used for small onsite medical O_2 delivery systems.

The non-cryogenic air separation methods use the gases physical property differences such as molecular size, structure, and mass. Each of the processes are based on adsorption equilibrium and permeation on adsorbents or membranes. The separation technology for chemicals and membranes are still developing. Chemical separation has material corrosion issues making it unsafe for personal medical use. Membranes struggle to produce high purity O_2 at ambient temperatures. Higher purities have been achieved in systems at high temperatures (+500 °C) making membranes inadequate and unsafe for personal medical use. The final option for gas separation and the preferred method in POC's is adsorption.

2.1.1. Adsorption based air separation

Adsorption is-based on the ability for a natural or synthetic material to preferentially adsorb one of the primary components that make up atmospheric air. In the case of a POC, nitrogen (N_2) must be adsorbed to deliver high purity O_2. The material typically used for this are zeolites, Smith (2000). Zeolites have a non-uniform electric field in the void spaces of the material causing a preferential adsorption of N_2 as the molecule can be polarised due to having a greater electrostatic quadrupolar moment.

When pressurised air is passed over a column of zeolite adsorbents. The N_2 is adsorbed on to the zeolite and an O_2 enriched product gas will be generated at the exit of the column. The adsorbed N_2 will need to be desorbed from the zeolite by lowering the pressure or raising the temperature in the column. This process has been developed through different cycles:

i. Thermal Swing Adsorption (TSA)

ii. Pressure swing adsorption (PSA)

iii. Vacuum pressure swing adsorption (VPSA)

The TSA process is the oldest and most completely developed cycling method Yang (1987). The column is purged with a preheated gas to raise the temperature for the desorption phase. As the heating of the gas is the time limiting factor of the cycle. The full cycle time for a TSA can range from several hours to over a day. TSA cycles are best used when the concentration of the desired adsorbed component is low and is more often used for purification purposes. The times involved for a cycle and the temperature required makes TSA an impracticable method for portable personal medical oxygen generation.

A PSA cycle to separate air for oxygen enrichment was first patented by Skarstrom in 1960. The schematic of the basic Skarstrom cycle for pressure swing adsorption is shown in Figure 2 with a Table of operation.

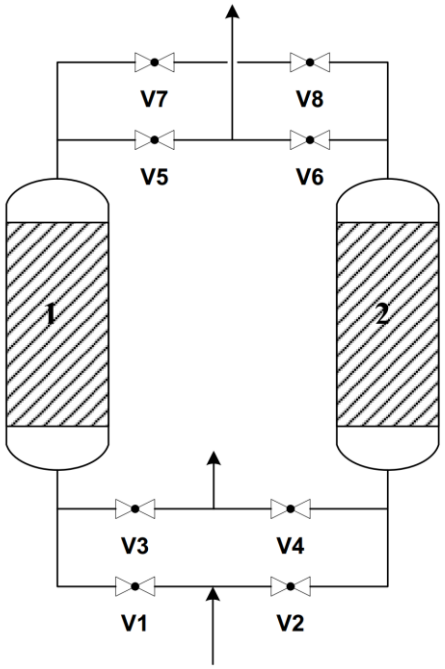

Step	V1	V2	V3	V4	V5	V6	V7	V8
Pressurisation	✓	X	X	✓	X	X	X	X
Adsorption	✓	X	X	✓	✓	X	✓	✓
Blow Down	X	✓	✓	X	X	X	X	X
Purge	X	✓	✓	X	✓	✓	✓	✓

Figure 2: Example Skarstrom Schematic and Valve Timing

The Skarstrom cycle consists of two columns filled with adsorbents and each column will go through four steps: pressurisation, adsorption, blowdown and purge. Both columns go through the four steps at different times. While column 1 is being pressurised by high pressure air from V1. Column 2 will be going through blowdown by opening V4 to atmosphere and letting the pressure in the column exhaust removing the adsorbed N_2. Column 1 will then move to the absorption step which will see oxygen enriched gas leave through V5. Concurrently column 2 will be going through the purge step by opening V5 and V6. This takes the enriched gas from column 1 and uses it to further remove adsorbed N_2 in column 2. The purge step is essential to achieve efficient separation. It ensures strongly adsorbed components are pushed back from the column outlet, so the enriched gas does not become contaminated in the next cycle. Column 1 will then go through the blowdown and purge steps while column 2 goes through the pressurisation and adsorption steps. The benefit of the two columns is that the timings can be balanced to allow for a constant outlet of enriched O_2.

Every air separation method is measured by three parameters: product purity, product recovery, and adsorbent productivity Yang (1987). When Skarstrom first proposed his cycle, it offered low separations of N_2 and O_2. However, the cycle did prove to be very efficient at drying gases and so the PSA cycle was commercially accepted. The release of the Skarstrom cycle initiated a new wave of research into PSA cycles and further development into the process variables: bed length, column pressure, inlet gas velocity, and cycle times to improve purity and recovery. Some of the major developments include but are not limited to, pressure equalisation steps which were used to lower power consumption, multi-bed PSA for continuous high flow outputs, and the development of a faster cycled PSA known a rapid pressure swing adsorption (RPSA), see papers reviewed in Appendix B.

RPSA systems are characterised by fast cycling (total cycle time <10s) and the use of small particles (0.3 mm - 0.7 mm). The benefits of using the RPSA is that most of the proposed designs use a single bed which simplifies on the process engineering. RPSA systems also offer a higher adsorbent productivity at an equal purity and recovery to PSA systems. The higher adsorbent productivity means less adsorbent is required to achieve the same output volume when compared to a PSA cycle. The downside to RPSA systems is that they are extremely complex due to the dynamics created in the fast cycling and the use of small particles, Yang (1987). So far, there are no companies advertising that they use RPSA cycles and the reason may be due to the difficulties in understanding the system. However, the possibility of reducing the volume of adsorbent used is a great opportunity.

Around the same time the Skarstrom cycle was patented, Guerin de Montgareuil and Domine (1964) patented a PSA cycle using a vacuum for desorption. A schematic detailing the vacuum PSA is shown in Figure 3. The steps followed the same sequences as the Skarstrom but instead of a purge step a vacuum would be used to further remove strongly adsorbed components.

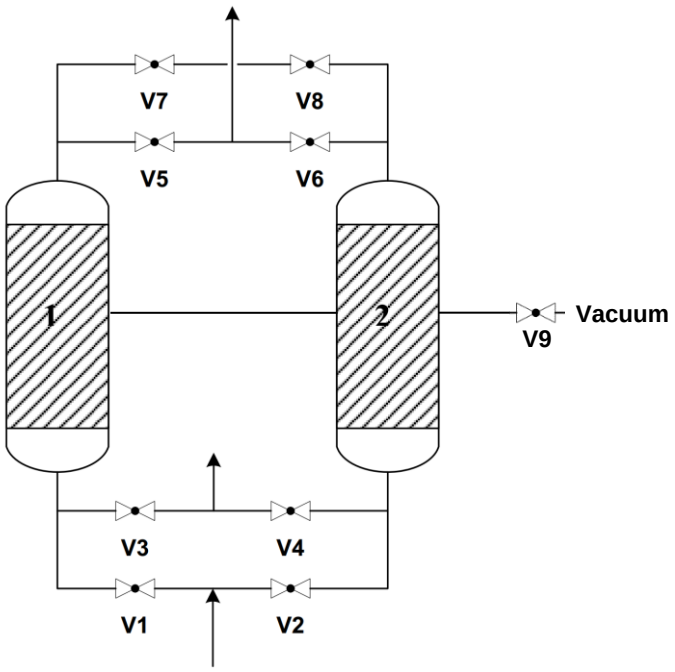

Figure 3: Example Guerin and Domine Schematic for VPSA

The VPSA proposed by Guerin and Domine yielded very impressive results obtaining a 98% oxygen purity (from argon free basis) at 51% recovery. The patent was assigned to Air Liquide who proceed to successfully commercialise the VPSA. So far VPSA technology has not been deployed in a POC due to the additional components required to generate a vacuum adding weight to the POC. Precision Medical claim to have a VPSA POC but at the time of writing, this was not commercially available on the market yet.

Therefore, PSA cycles have been the favored commercial method to generate oxygen in POC devices.

2.1.2. Nitrogen Selective Adsorbents

The critical step in designing any gas separation process is the right selection of adsorbent to be used. The critical factors to consider are:

i. The adsorbent capacity. This determines the amount of adsorbent required for the separation effecting size and weight.

ii. The selectivity. For a POC the adsorbent should have a preferential selection towards N_2.

iii. Kinetics of adsorption, which determine how quickly N_2 is adsorbed and desorbed. This can be in competition with adsorbent capacity per unit volume with a highly porous adsorbent material allowing high diffusional rates, but at the expense of sacrificing adsorbent internal surface area onto which the N_2 can adsorb.

iv. Another consideration should be the bulk density for crush strength in minimising attrition and dust generation.

As discussed in the previous section, zeolites are the industry preferred adsorbent for oxygen production for their high affinity to N_2.

Zeolites are a crystalline aluminosilicate with a framework of tetrahedral silicon SiO_4 and tetrahedral aluminium AlO_4. Using oxygen molecules, the primary units can be assembled into various arrangements to form open crystal lattices. The aluminium atoms create negative charges on the framework that must be balanced with an exchangeable cation site, Ruthven (1984). Zeolite has an non-uniform electrostatic charge field and the different quadrupole moments of N_2 and O_2 means N_2 preferentially adsorb into the pores. However, N_2 is not the only molecule to have a high affinity towards zeolite. Both water (H_2O) and carbon dioxide (CO_2) have high attraction to zeolite and can become strongly adsorbed permanently lowering the capacity of the zeolite and dropping the efficiency of a system. To protect zeolite by performing the air separation it is common practice in industry to use a material which will capture the H_2O and CO_2 before it reaches the zeolite. Typical adsorbents used for this are activated alumina, silica gel and sodium-based zeolites (NaX).

2.2. Rapid Cycling

An advancement in PSA technology was the invention of quicker cycling PSA systems known as Rapid PSA or Pulsed PSA. The first PPSA was proposed by Turnock and Kaldec (1971) for the separation of nitrogen from a nitrogen-methane mixture. Using a simple two-step process of feed and exhaust. They reached the conclusion that rapid cycling improved the nitrogen enrichment but at a very poor recovery. With poor recovery the system will require more adsorbent material to achieve the desired output. While the recovery was so low this made PPSA cycling unviable commercially.

Later, Jones (1980) patented the RPSA using a three-step process. A simple schematic detailing of the three-step RPSA system is shown below in Figure 4 along with a Table of operation. The system consists of one column packed with small particle adsorbents and typically has three steps: adsorption, delay and desorption. The cycle starts with V1 opening and allowing feed gas to pass through the column. Enriched gas will exit through V3. There is a short delay step with all three valves closed before V2 opens to allow the adsorbed gas to desorb under atmospheric pressure.

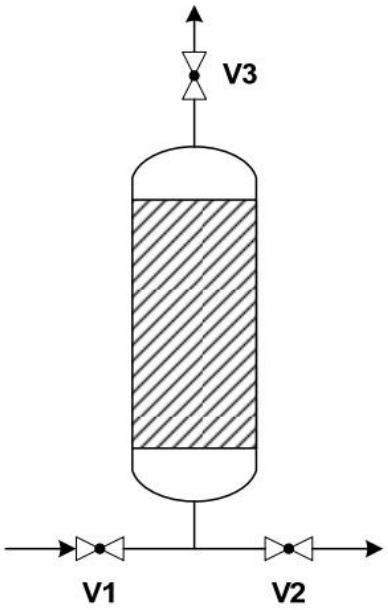

Step	V1	V2	V3
Adsorption	✓	X	✓
Delay	X	X	✓
Desorption	X	✓	✓

Figure 4: Example RPSA Schematic and Valve Timing

Jones (1980) outlined the important characteristic of an RPSA and what is vital to make the system viable-

i. Small particle adsorbents (0.3 mm - 0.7 mm). The use of small particle adsorbents is necessary to provide the required flow resistance in the system. It is important to understand the pressure drop in a column to obtain the required resistance. Pressure drop and small particles are explored further in Section 2.5. It was also highlighted that the pressure drop will have a direct impact on the power consumption of the

system. The higher the pressure drop the more powerful the compressor affects the size and weight of the system.

ii. Fast cycling (<10 seconds). Fast cycling can only be achieved when using small particles. The smaller particles reduce the diffusional path and increases the external surface area per unit volume of packing. This reduces the mass transfer resistance for the strongly adsorbed component of the absorbate. Resistance to mass transfer are discussed further in Section 2.6.

iii. The use of a single column is suggested to reduce the number of valves and make the process control easier.

iv. The timings of the three steps outlined above and varying these can have a dramatic change on the productivity of the adsorbent and the recovery of the product. The adsorbent step must remain short to avoid product contamination from the strongly adsorbing component due to the high interstitial velocities caused by the pressure drop. The desorption step must be longer than the adsorption step to allow the adsorbent to fully regenerate.

v. The length of the column will also have a direct effect on the productivity of the adsorbent and the recovery of the product. Jones (1980), managed to improve on Turnocks results by adding the additional step, reducing the length of the column used, and by using smaller particles.

Jones (1980) using the three-step RPSA process managed to achieve a five-fold increase in oxygen production per unit mass of adsorbent compared to the original Skarstom PSA cycle. This leads to a reduction in the volume of adsorbent required to achieve the same output. This encouraged a new wave of research into RPSA and PPSA systems which is summarised in Appendix B.

2.2.1. Summary of RPSA review

From the literature found over the last 30 years it is hard to find a common theory as the process has so many varying parameters which change on every paper reviewed in Appendix B. The column sizes vary from lengths of 127 mm – 1524 mm with diameters of 31.75 mm – 300 mm. The flows vary from 0.02 Lpm – 200 Lpm. The particle sizes vary from 0.001 mm - 0.7 mm. The cycle times also vary from 0.05 seconds – 10 seconds. There is also little

evidence of the same parameters from an experiment or theoretical study being repeated to prove theories.

As many of the papers do not contain all the information needed to replicate a study. A paper by Chai (2011) was the first to propose a column size that could feasibly be used within a portable oxygen concentrator. The Chai paper provides sufficient information for the bases of an experiment and allow an initial investigation into the understanding of RPSA cycles in small columns.

A paper by Rama (2014) provides the most details about their cycle and utilises a small column. However, the paper requires an input flow rate of 110 Lpm. It should be noted that this would never be possible with a POC as a compressor to achieve this would weigh around 2,5 kg.

Nearly all papers propose the use of a single column and continuous input flow which is buffered through a surge tank to account for switching between steps of the process. This proposed method will have to be scrutinised to verify if the required size of a surge tank is a benefit to the system or would a second bed, like the Skarstrom cycle, be a better proposal to keep the compressor running and possibly power consumption lower.

2.3. Ultra-Rapid Cycling

Ultra-Rapid Pressure Swing Adsorption (URPSA) is a development of the RPSA concept where a very thin bed of adsorbent particles is subject to a cycling process like the RPSA but even quicker. The concept is the quicker cycling will further improve the adsorbent productivity.

The concept was first proposed by Suzuki *et al.* (1996) using a piston cylinder assembly which has a column packed with adsorbent particles in it. They concluded that oxygen productivity was very high, but the oxygen recovery was very low. The same piston URPSA systems were further developed by Singh and Jones (1997) and Arvind (2002). Using Zeolite 13X adsorbent and studying the process parameters they concluded that piston URPSA process was better than the standard PSA and comparable to the RPSA.

The URPSA process was developed further by Kopaygorodsky (2002) by using the URPSA sizes and timings but not with a piston. Kopaygorodsky used a single column 20 mm thick with a diameter of 200 mm which was packed with 0.001mm particles and went back to the two-step process of pressurisation and depressurisation. Using this set-up, a purity of 85%

oxygen was achieved with a recovery of 56%. This is an improvement on the standard PSA system and is comparable to the RPSA process. The benefit of the URPSA is a further reduction in the volume of adsorbent compared to the RPSA. Kopaygorodsky only simulated this set-up leaving a window for an experiment to further prove the study.

Further investigations into URPSA revealed a patent by Galbraith *et al.* (2011) which proposes a portable oxygen concentrator with a small column using <15g of aluminum phosphate adsorbent particles sized 0.06 to 0.12 mm to generate 85-92% oxygen at a flow rate of 0.8 Lpm. The patent shows that an increase in the cycling frequency decreased the volume of adsorbent required. There is little information regarding how the information in the patent was generated and leaves a window of opportunity for an experiment to prove the proposed theory.

2.4. Rapid Vacuum Pressure Swing

One study demonstrates the addition of a vacuum to the RPSA cycle by Zhu *et al.* (2016). Through simulation and experiment of a VRPSA cycle Zhu achieved 0.75 Lpm of 90% O_2 from compressed air. The adsorption pressure was 240Kpa whilst the desorption pressure was 60Kpa. Interestingly the addition of using intermediate gas generated from the product output to pressurise the column improved the recovery by 5%.

With little information about vacuums included on RPSA and URPSA cycles there is an opportunity to develop the system further. To review how a vacuum can be applied in a small POC system where weight is a big factor so having two compressors, as used by Zhu, would not be a favorable option.

2.5. Pressure Drop

URPSA and RPSA systems use very small particles densely packed together in a column. This generates a resistance to fluid flow creating pressure drop across the column. The effects of pressure drop on fluid dynamics and the fast-cycling process has been well researched and will be reviewed in this section.

Pressure drop was calculated across all the reviewed papers using steady-state momentum Equation – either Darcy (laminar flow) or Ergun (turbulent flow). The validity of using Darcy or Ergun's Equation for determining pressure drop was experimentally proven by Sereno (1993) and Todd (2005).

The first pressure drop Equation was developed by Darcy (1856) while measuring pressure drop over a porous medium to determine the average velocity at which fluid passed through it and is given as:

$$\frac{\Delta p}{L} = \frac{u_Z}{K_P} = \frac{\varepsilon_b^2 v_z}{K_P} \tag{1}$$

The pressure drop along a unit length is given as $\frac{\Delta p}{L}$, u_z is the average velocity (superficial velocity) based on the total area of packing and K_p is a constant that measures permeability of the porous media. ε_b is the overall bed voidage and v_z is the velocity of the fluid within the porous media (interstitial velocity) assuming the tortuosity is equal to 1.0.

As larger particles and higher-pressure drops were experimentally studied the linear relationship began to break down. Instead, the function follows a quadratic relationship between velocity and pressure drop.

$$\frac{\Delta p}{L} = \frac{u_Z|u_z|}{K_{P2}} = \frac{\varepsilon_b^2 v_z|v_z|}{K_{P2}} \tag{2}$$

As such, it has become practice to combine Equation (1) and Equation (2) to get an accurate pressure drop over a wider range of velocities Lage (1998). Giving Darcys Equation its final form as:

$$\frac{\Delta p}{L} = \frac{u_Z}{K_P} + \frac{u_Z|u_z|}{K_{P2}} = \frac{\varepsilon_b v_z}{K_P} + \frac{\varepsilon_b^2 v_z|v_z|}{K_{P2}} \tag{3}$$

Ergun (1952) through extensive experimental data covered a range of particle sizes and flows to derive Equations for the viscous permeability of the column (K_p) and inertial permeability of the column (K_{p2}).

$$K_p = \frac{\varepsilon_b^3 d_p^2}{150(1-\varepsilon_b)^2 \eta} \tag{4a}$$

$$K_{p2} = \frac{\varepsilon_b^3 d_p}{1.75(1-\varepsilon_b)\rho} \tag{4b}$$

Equation (4a and b) are combined to generate what is known as the Ergun Equation to determine pressure drop through packed columns.

$$-\frac{\Delta p}{L} = 150\frac{(1-\varepsilon_b)^2}{\varepsilon_b^3}\frac{\eta u_z}{d_p^2} + 1.75\frac{(1-\varepsilon_b)}{\varepsilon_b^3}\frac{\rho u_z |u_z|}{d_p} \tag{5}$$

The terms in the Ergun Equation are: $\frac{\Delta p}{L}$ is the pressure drop along a unit length; ε_b is the overall bed voidage; η is the fluid velocity; u_z is the average velocity (superficial velocity) based on the total area of packing; d_p is the diameter of the particle; and , ρ is the total density of the fluid. The constants of 150 and 1.75 were determined through Ergun's experimental data. However, it has been suggested that the constants can change depending on the particles used as observed by Todd (2005). For LiLSX particles Todd observed a viscous coefficient of 154 which is in good agreement with Ergun. However, the experimental data showed a kinetic coefficient of 1.47 which is smaller than Ergun's results and much smaller than literature estimates for smooth particles which is between 1.75 and 1.8.

Understanding pressure drop in a column is going to be critical when designing a URPSA system. The smaller columns and higher gas throughputs of a URPSA system result in higher pressure drop leading to an increase in interstitial velocity. This has three impacts -

This increases the axial pressure gradient until a limit is reached. When this threshold is reached fluidization occurs resulting in rapid attrition of the particle Todd (2005).

It can lead to early breakthrough of concentration Sundaram (1988), Kikkinides (1993) and Yang (1998).

It will also spread the mass transfer zone Yang (1998) due to a decrease in driving of the mass transfer Rama (2010).

2.6. Dispersive Resistances

It is important to review dispersive resistances when considering any PSA adsorbent system as it has a vital impact on the gas flow dynamics and dispersing the mass transfer zone. Without good estimations in place for dispersive resistances it will have a direct negative impact on simulating.

The mass balance Equation for gas flow through a packed bed is given as:

$$\frac{\partial c_i}{\partial t} + \left(\frac{\rho_b}{\varepsilon_b}\right)\frac{\partial n_i}{\partial t} + \frac{\partial (v_z c_i)}{\partial z} = \frac{\partial}{\partial z}\left[D_L c \frac{\partial y_i}{\partial z}\right] \tag{6}$$

with the Equation describing the following: gas phase accumulation, adsorption rate convection, and axial dispersion. If the gas concentration along the bed does not change (i.e isothermal and isobaric) then this can be written as:

$$\frac{\partial c_i}{\partial t} + \left(\frac{\rho_b}{\varepsilon_b}\right)\frac{\partial n_i}{\partial t} + \frac{\partial (v_z c_i)}{\partial z} = D_L \frac{\partial^2 c_i}{\partial z^2} \tag{7}$$

The adsorption rate can be described using the linear driving force (LDF) model which is expressed as:

$$\frac{\partial n_i}{\partial t} = k_i (n_i^* - n_i) \tag{8}$$

where n^* is the equilibrium value of component i in the adsorbed phase at a given fluid phase concentration and n is the adsorbed phase concentration of component i, both averaged over an adsorbent particle. The mass transfer coefficient (MTC), k_i, is where the dispersive resistances are considered in the material balance Equation. For a spherical particle this is given by Ruthven (1984) as:

$$\frac{1}{k_i} = \frac{Kr_p}{3k_f} + \frac{Kr_p^2}{15\varepsilon_p D_{pi}} + \frac{r_c^2}{15D_{ci}} \tag{9}$$

with the three terms representing mass transfer in the film, macropore and micropore resistances. Not all resistances are considered important to the mass transfer coefficient due to their small or negligible effects. It is here where literature differs on what resistance or resistances have the largest effect and should or should not be included.

Large diameter particles (>2 mm) zeolite are known to display a large mass transfer resistance in the macropores due to the distance molecules must travel into the particle. As this is the overriding resistance in large particle columns, a mass transfer rate controlled by macropore resistance is typically assumed in the mass balance Equation Haq and Ruthven (1986); Ruthven and Xu (1993). If the macropore term is considered controlling the above Equation (9) simplifies to:

$$k_i = \frac{15\epsilon_p D_{pi}}{Kr_p^2} \tag{10}$$

It should be noted that the particle radius as the denominator means that as the particle gets smaller the MTC gets higher which should give a more productive process, which is the basis for URPSA. As outlined in the introduction, URPSA processes use small particles in the region of 0.3-0.7mm in diameter. The reduction in particle size is intended to allow quicker cycling through reducing the macropore diffusion resistance by both shortening the diffusional path and increasing the external surface area per unit volume of packing. This shifts the mass transfer rate controlling mechanism to effects that are external of the particle such as axial dispersion Zhong *et al.*. (2010).

Axial dispersion is currently represented in the mass balance Equation (6) as D_L. In its simplest form is given as Ruthven (1984):

$$D_L = \gamma_1 D_m + \gamma_2 v_z d_p \tag{11}$$

The first term represents the molecular diffusion which is important at low flows and the second term represents the convection diffusion which is important at high flows.

Axial dispersion is described by Ruthven (1984) as the splitting and recombining of the molecules as they pass through the bed. A more detailed explanation comes from Gunn (1969) who considers the bed to have two streams, fast and slow. The fast stream is the molecules quickly passing through the bed and the slow stream is the molecules that are trapped behind particles. The molecules can move in and out of the streams as they pass through the bed. The molecules in the fast stream are what increase the axial dispersion coefficient.

Y1 and Y2 are constants and are typically estimated as 0.7 which is the inverse of the touristy factor and 0.5 which is the inverse of the limiting Peclet number at high Reynolds number which has been observed in Literature from several authors as 2 as shown in Equation 12. The Peclet number is defined as:

$$\mathrm{Pe} = \frac{v_z d_p}{D_L} \tag{12}$$

And the Reynolds number is defined as:

$$\mathrm{Re} = \frac{\varepsilon_b v_z d_p}{D_L} = \frac{u_z d_p}{D_L} \tag{13}$$

Table 3: Langer (1987) and Ruthven (1984) Peclet Number Review

Paper	$\frac{x}{d_R}$	d_p**(mm)**	τ	β	$\mathbf{Pe}_\infty$
McHenry-Wilhelm	18	3.23			1.88
Edwards-Richardson	10	0.377-6.07	0.73	13	2.0
Evans-Kenney	164	1.96	0.67	10	2.0
Urban-Gomezplata	16	6-16	0.73	19	2.0
	16	1.5	0.73	10	1.0
Scott Lee-Papa	59	16	0.75	29	2.0
	63	7/8.7	0.64	39	2.0
	53	8.7	0.57	42	2.0
Suzuki-Smith	204	0.1-0.8	Not Provided	Not Provided	0.13-0.77

Table 3: Langer (1987) and Ruthven (1984) (Continued)

Paper	$\frac{x}{d_R}$	d_p(mm)	τ	β	Pe_∞
Van Deemter u.a.	408	0.056	Not Provided	Not Provided	0.125
		0.225	Not Provided	Not Provided	0.333
Kawazoe u.a.	97	0.67	Not Provided	Not Provided	0.51
	45	1.41	Not Provided	Not Provided	1.20

The limiting Peclet number of 2 has been shown by the above authors to be generally consistent with larger particles (>3 mm). The data for smaller particles (<3 mm) and in the range of intermediate Reynolds numbers show much smaller Peclet numbers giving an increase in the axial dispersion coefficient. The increase in axial dispersion coefficient has been attributed to small particles forming agglomerates which act as large particles affecting the fluid flow. The agglomerates are a consequence of large interaction forces between particles Moulijn and Vanswaaji (1976).

With a clear correlation between axial dispersion and particle diameter being suggested through literature, Langer *et al.* (1978) proposed Equation (14) as a more accurate alternative to Equation (11).

$$D_L = \gamma_1 D_m + \frac{d_p \bar{u}_z}{Pe_\infty \left(1 + \frac{\beta \gamma_1 D_m}{d_p \bar{u}_z}\right)}$$

$$\mathrm{Pe}_\infty = 2, \qquad d_p \geq 3\ mm$$

$$\mathrm{Pe}_\infty = 3.35\left(\frac{d_p}{2}\right), \qquad d_p \geq 3\ mm \tag{14}$$

$$\gamma_1 = 0.45 + 0.55\varepsilon$$

$$\beta = 0.7 - 42$$

As axial dispersion is contributing to the dispersion of the MTZ in small particles it can be included in Equation (9) as contributing to the overall MTC. This is only possible when a linear isotherm and the LDF model is used for the transfer rate Wu (2014).

$$\frac{1}{k_{overall}} = \frac{KD_L}{u_z^2}\left(\frac{1-\varepsilon_b}{\varepsilon_b}\right) + \left(\frac{Kr_p^2}{15\varepsilon_p D_{pi}}\right) + \left(\frac{Kr_p}{3k_f}\right) + \left(\frac{r_c^2}{15D_{ci}}\right) \quad (15)$$

Equation (15) is often referred to as the linear approximation Haq and Ruthven (1986); Ruthven and Xu (1993).

Equation (15) will replace Equation (9) for generating the MTC. The axial dispersion term in the mass balance Equation (6) is dropped and this turns into a plug flow model Ruthven (1984).

It needs to be considered that early studies of axial dispersion, including papers used in Table 3, mainly used non-adsorbing particles to monitor axial dispersion and to limit additional contributing factors. It has been assumed that the models for axial dispersion which were derived using non-porous particles can also be used on porous particles. This may not be strictly true though as unusually high axial dispersion coefficients were witnessed by Suzuki and Smith (1971), when using porous particles. This was also observed by Wakao (1978) at low Reynolds numbers. The higher axial dispersion witnessed by Wakao is attributed to direct transport through the particle which is a result of an asymmetric concentration profile around the particle. At high Reynolds numbers there is enough turbulent mixing to assume a uniform concentration boundary at the particle. It can be assumed that the effects reported by Wakao will not affect this study as URPSA process operate at high Reynolds numbers. This is further confirmed by an experimental study performed by Alpay (1994) who studied the effect of reducing porous particle sizes to find an optimum size for air separation. During the study the above Langer Equation (14) for axial dispersion was used. In the study it was also noted that the Equation was derived using non-porous particles and some error may occur which is associated with transport through the solid. However, Alpay concluded that the Langer Equation was adequate to predicted axial dispersion. This suggests that the Langer Equation (14) though derived from non-porous particles applies to porous particles at high Reynolds numbers.

A dispersive resistance not covered so far as it is typically considered negligible for larger particles is skin resistance. Skin resistance comes from the manufacturing process of particles. When shaping particles, a crystalline structure can form at the skin providing extra

resistance to flow through the particles. The assumption that skin resistance is negligible needs to be confirmed for smaller particles.

Wu (2014) explored all dispersive resistance for small particles and their effects on the mass transfer coefficient. Wu suggests that skin resistance at the binder surface has the largest effect on the mass transfer coefficient. More so than axial dispersion which had been the focus of previous studies. This was questioned by Moran (2018) who experimentally studied the effect of axial dispersion and skin resistance on MTC. By using literature, Moran derived varying MTC curves at increasing Reynolds numbers to highlight the effect different dispersive resistances will have. Moran's experimental data showed that considering particle size as part of the axial dispersion correlation was the closest at predicting the MTC and that skin resistance did not have as large an effect as Wu suggests.

If the literature cited throughout this section is correct axial dispersion effects increase significantly with small particles and plays a significant role in dispersing the mass transfer zone. To generate data for adsorption simulations experimental breakthrough studies will have to be performed to reasonably estimate axial dispersion. Failing to do so will lead to inaccurate results. Perhaps from the data generated an agreement may be found with previous literature to allow for standard correlations to be used in future.

2.7. Wall Effects

None of the literature cited and reviewed consider wall effects fully. To not consider wall effects, a column to diameter ratio above a common accepted threshold of 20 is used as a method to prevent wall effects.

However, recent papers have considered such thresholds and common rules to in fact be incorrect. Son *et al.* (2019), used existing correlations to predict axial dispersion and found them to grossly under predict the observed axial dispersions due to wall effects.

I acknowledge that due to the sizes of columns required in a small POC it would be hard to meet common rules and thresholds. Also, these rules may not be true. The focus of this research will be to experimentally test an RPSA cycle. As such, break through results can be matched to simulation breakthroughs to help determine accurate axial dispersion and MTC numbers. To fully consider wall effects in a small column in an RPSA cycle is beyond the scope of this study.

2.8. Patents

A patent survey was conducted to review inventions claiming to use rapid pressure swing adsorption in portable oxygen concentrators. The purpose of the survey is to understand state-of-the-art technology for rapid pressure swing adsorption and portable oxygen concentrators which could be commercialized or impact the contemporary research being developed in this doctoral research.

Rapid pressure swing adsorption has been referenced in around ~400 patents with Russel L Jones releasing the first back in 1978. The results can be focused down to ~25 patents by looking at the ones relevant to “oxygen” separation. Much like the work carried out in literature, the patents focus on large scale production using large columns.

To narrow down the results of the search to target column scales this research will focus on the following search terms that were used: "rapid pressure swing adsorption" "portable oxygen concentrator", yielded 0 results of relevance. The search terms "rapid pressure swing adsorption" "oxygen concentrator", yielded the following three results.

- Weihai Weigao Haisheng Medical Equipment CO Ltd (2018), describes a “kind of medical oxygen concentrator based on rapid pressure swing adsorption”. The patent describes an oxygen concentrator which supplies hospital beds and uses 0.5 Mpa which is 72.5 psi. An unrealistic pressure to achieve in a portable oxygen concentrator due to the size of compressor require to achieve the desired pressure.
- Lee *et al..*, (2004), describes using a rapid pressure swing adsorption process to be applied in a small size oxygen concentrator. The patent details the cycle steps and process. It does not give any details on size, weight, timing, and pressures. It is also noted that the patent is anticipated to expire in February 2024 so should cause no concern to this research.
- Kulish *et al..*, (2000) describes a rapid pressure swing adsorption process for an oxygen concentrator. The patents focus on the concentrator using 3/6 sieve beds in a rotating carousel and the design of the manifold to mount the sieves. Some details are provided around the expected sizes and device capability, but not specifics. As this patent was released in 2000 it has expired and as it is focused on the sieve carousel design there is no concern about it interfering with this research.

Other terms that could be considered as synonyms to rapid were checked: “fast”, “quick”, and “ultra”. The terms, fast and quick, did not produce any patents of relevance. Instead, it produced patents where sentences included: “fasteners”, “fast flow”, “quick-connect”, and “quick repair”. The search terms with ultra, provided the following patent.

- Galbraith *et al.*. (2011) describes the design of a portable oxygen concentrator using an Ultra PSA with cycle times of less than a second. The concentrator in the patent can achieve through a unique design of valving oxygen purities of 85-92% and flow rates of 0.8 Lpm with ~15 g of adsorbent. The patent also claims that with lower weight, faster cycles of 0.15 seconds can be achieved. This patent is of interest as it will have to be reviewed against the end results of this research.

As before the commercialisation of a product, a search for prior art will have to be conducted to avoid legal infringement. This would ideally be conducted with lawyers specialising in the subject to ensure compliance with the market.

2.9. Portable Oxygen Concentrator Market Review

A complete review of both the portable and stationary O_2 concentrator market has been performed, see all data in Appendix A. Figure 5 presents the latest devices on offer from each O_2 concentrator manufacturer and the circled area shows the weight difference between a portable concentrator and a stationary concentrator. Figure 6 shows the output to weight ratio for the lightest POCs on the market. The four devices giving the highest output to weight ratio are the Airsep Focus, Inogen G4, Vbox Trooper and the 3B Products Aer X. The Airsep Focus is misleading; it is advertised as 0.8 kg but this is not inclusive of any batteries which weigh 0.2 kg each and must be worn on a 0.8 kg battery belt. When taking this into consideration, the Airsep Focus has one of the lowest output to weight ratios. The Vbox trooper looked very impressive but was no longer available for purchase, and the technology was purchased by 3B products. At the time of writing, the 3B products Aer X has not yet been released. This leaves the Inogen G4, which weighs 1.2 kg, has a battery life of up to 5 hours, and can output 0.63 Lpm of high purity O_2 setting this device as a leader in the POC market.

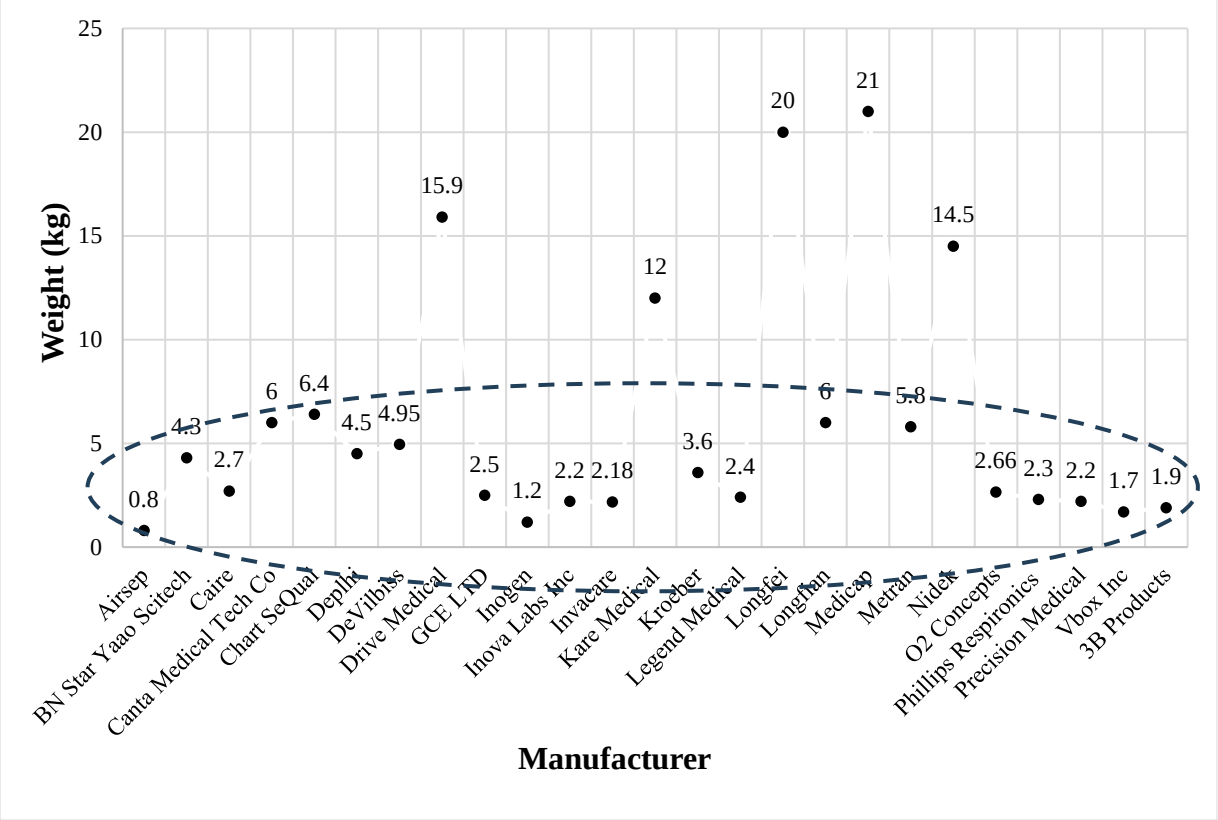

Figure 5: Oxygen Concentrator Market Review

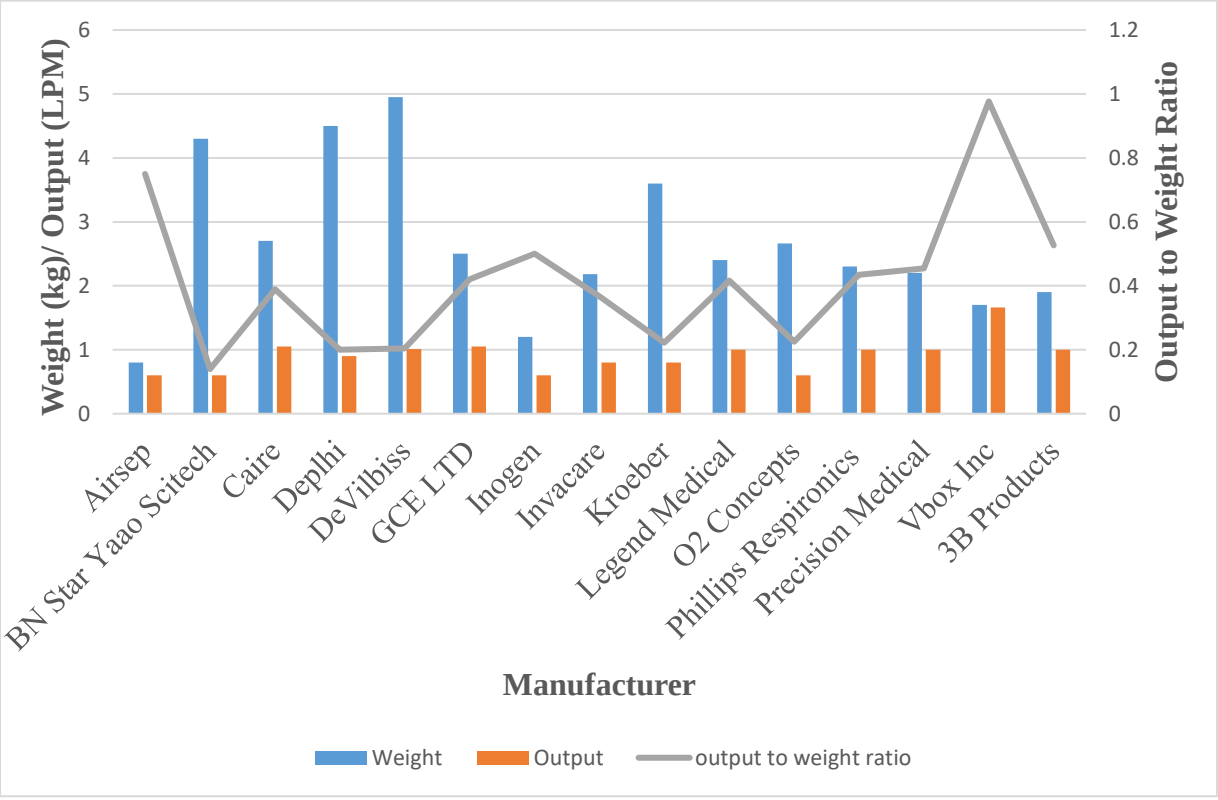

Figure 6: Output to Weight Ratio of the Lightest POCs Determined from the Oxygen Concentrator Market Review

2.10. Portable Oxygen Concentrator

Like most of the industry, POC devices operate a version of the Skarstrom cycle. A POC typically consist of a minimum of two columns, a compressor and multiple valves to control the pressure cycling and flow sequences required. The columns will be filled with enough zeolite-based adsorbent to produce a desired O_2 volume and a desiccant to remove H_2O and CO_2 from atmospheric air.

The volume of zeolite and the compressor size which are the main contributors to the weight of a device are directly related to the productivity and recovery of the adsorbent, Jones (1980). Minimising POC devices using the Skarstrom cycle has clearly reached a limit with all major companies shown in Figure 6 achieving a similar output to weight ratio.

To dramatically reduce the weight of a POC and improve a user's lifestyle a different approach to gas separation will have to be made.

The RPSA process discussed in Section 2.2 is the best opportunity to reduce the weight of a POC. The systems which have been proposed so far in literature show that adsorbent productivity can be improved five times over that of the Skarstrom cycle, Jones (1980). This would suggest that RPSA systems can greatly reduce the volume of adsorbent to achieve the same outputs. The systems proposed have been designed to have one column further reducing the weight as less valving is required.

The RPSA system has a similar recovery to the Skarstrom cycle so the size of the compressor cannot be improved. However, VPSA systems benefit from a higher recovery rate than the Skarstrom cycle.

2.11. Literature Review Conclusion

The aim of the literature review was to explore gas separation methods that could be used to reduce the weight of portable oxygen concentrators. The literature reviewed explored the background and basic theories of PSA's, alongside rapid cycling. From the review, it can be concluded that RPSA cycling has been used to reduce the volume of adsorbent required in gas production systems. As such, the following research question can be proposed:

'Can using the RPSA cycle significantly improve oxygen yield per unit volume of adsorbent allowing the development of a small, light POC?'

The gap in the reviewed literature is the use of RPSA in small bed sizes or oxygen concentrators. The result, the proposed research being carried out on RPSA in small bed sizes for the use of POC's is novel.

2.11.1. Research Question Target

Section 2.9 reviewed the POC market and concluded that the Inogen G5 was the best performing device with regards to output vs weight. This metric took into consideration multiple aspects of the POC. For example, batteries, motor, valves, plastic, etc. This research is just focusing on the development of a pressure swing cycle. As such, the review of the Inogen G5 and those similar on the market can be taken further. By reviewing the weight of the adsorbent to the device output, a more accurate measure of "device output per gram of adsorbent" can be created. This will allow for a more accurate measure of performance to be created by comparing "device output per gram of adsorbent". This analysis is performed in Table 4 identifying that the Inogen G4 has the best output to adsorbent weight ratio.

Table 4: Review of Device Output in ml per gram from the Lightest Devices Identified in the Oxygen Concentrator Market Review

POC Device	Zeolite Mass (g)	Device Output (ml)	Device Output (ml per g)
Inogen G4	152	630	4.14
Inogen G5	266	1260	4.73
Zen-O lite	220	1050	4.77
Zen-O	460	2000	4.34

The question of: *Can using the RPSA cycle significantly improve oxygen yield per unit volume of adsorbent allowing the development of a small, light POC?* It can be further improved with the target to produce a better output per gram of adsorbent than the current POC market and achieve the industry expected oxygen purity of ~90%.

3. METHODS AND MATERIALS

Chapter 3 provides the methods and materials used for the experiments which will be discussed in chapter 6. The adsorbent being used across all experiments is detailed in Section 5.1. In Section 5.2, the equipment and process are outlined to understand an RPSA from an existing paper and develop a new RPSA.

To support the development of the RPSA cycle, three additional experiments were carried out. In Section 5.3 the equipment and process are outlined for breakthrough testing. In section 3.4 the equipment and process are outlined for crush testing. In Section 3.5 the equipment and process are outlined for thermogravimetric analysis experiments.

3.1. Adsorbent

The adsorbent used for experiments was purchased from ZeoChem AG (Joweid 5, CH-8630 Ruti). The adsorbent is a lithium-based Zeolite with the product name: Zeox Z12-49.

3.2. RPSA Gas Separation Methodology

The purpose of this experiment is to explore RPSA gas separation methodologies detailed in past papers. Then to develop the knowledge from the experiments to create a rapid cycle that increases the oxygen yield per unit of adsorbent for use within a portable oxygen concentrator.

3.2.1. Apparatus

- Pressurised Air
- ZeoChem Samples Zeox Z12-49 (Zurich 8630, Switzerland)
- Calibrated Alicat 0-10 Lpm mass flow meter (Tucson, AZ, US)
- Calibrated Alicat 0-10 Lpm mass flow meter (Tucson, AZ, US)
- Calibrated Alicat 100 SCCM mass flow meter (Tucson, AZ, US)
- Restrictor – IMI Norgren T1000C1800 B7227 (Hollingworth UK)
- 3/2 solenoid valve – Mac Valves MOD 8955 (Wixom, Michigan, US)
- 2/2 solenoid valve – Mac Valves MOD 8954 (Wixom, Michigan, US)
- Swagelok needle valve x2 – SS-1RS6MM (Warrington, UK)
- 3D printed valve block x 3
- SST Sensing Oxygen Sesnor part number O2S-FR-T5 5 (Coatbridge, UK, ML5 4NS)
- Arduino Uno board and 8 Channel Relay Module (Somerville, Massachusetts, US)

- Computer running:
    - Minitab (Coventry, UK)
    - Oxygen Sensor Software by SST Sensing (Coatbridge, UK, ML5 4NS)
    - Arduino Cloud Software, (Somerville, Massachusetts, US)
    - Alicat logging system. Propriety software written in Python by GCE (Haydock, UK)

3.2.2. Apparatus Layout

*Mass Flow and Pressure Sensor

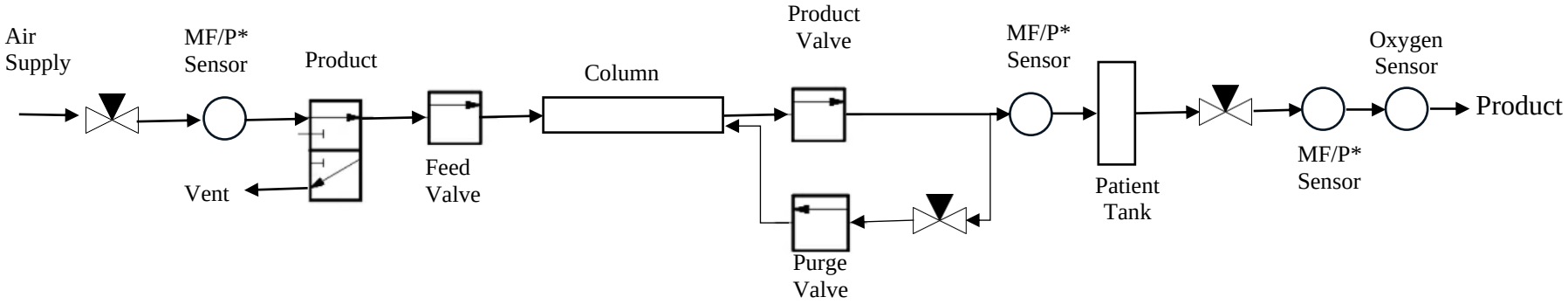

Figure 7: RPSA Development Schematic Layout

3.2.3. Process

3.2.3.1. RPSA Methodologies Experiment

The purpose of this experiment is to examine past literature RPSA results to further understand the technology.

The step-by-step of the process is as follows:

1. The equipment will be connected as per layout in Figure 7.
    a) The column length used was fixed to 110 mm in length and 6.4 mm in diameter.
2. The mass flow sensors and oxygen sensors will be powered on.
3. The oxygen sensor was powered on and allowed to warm. The warm-up time includes self-calibration to air. The supporting software for the oxygen sensor displays calibration and warm-up time. The sensor output is checked with 100% and 92% oxygen to ensure the readings are accurate.
4. Once set for an experiment session, the calibration and checks do not need to be performed again. It is only repeated when the sensor has been turned off and on.
5. The pressurised air and restrictor will be set to only allow a supply of 2.5 Lpm at 29 psi.
6. The column under review will be filled with “fresh” adsorbent.
    a) Note: The adsorbent will come straight from the manufacturer and remain sealed/ uncontaminated up to testing to ensure the adsorbent has not been degraded.
    b) The adsorbent will be resealed in a nitrogen atmosphere when being stored as per the suppliers’ recommendations.
    c) When tests are conducted back-to-back. Helium will be passed through the column to purge the adsorbent and clean it of any containment. The helium will be passed through the column at a rate of 0.25 Lpm for three minutes.
7. The timings for the solenoid valves were set in the Arduino code. The valves from MAC Valves can operate at 2000Hz. The specific valve supplied from MAC Valves to GCE has been confirmed through private conversation (GCE) that the valves used in the experiment can operate at 100 times the speed used in the experiment.
    a) Product valve
    b) Feed valve

c) Product valve

d) Purge valve

8. All equipment has been prepared to start an experiment. The mass flow sensors and oxygen sensors are set to “recording” in their associated software.
9. The valve to the airline is opened. It remains open until the oxygen purity has peaked and returned to its starting air value. When this happens, the valve is closed.
10. The mass flow sensors and oxygen sensor recordings are stopped.
11. The experiment has finished.

3.2.3.2. RPSA Development

The purpose of this experiment is to develop an RPSA cycle that can be utilized for use in a portable oxygen concentrator. Much of the experiment will follow the same steps as the RPSA methodologies experiment outlined in section 3.2.3.1 as the process to start testing and set-up will be very similar. The main difference will be from step 7 onwards when the valve controls differ.

The step-by-step of the process is as follows:

1. The equipment will be connected as per layout in Figure 7.
    a) The column length is determined by the breakthrough experiments.
2. The mass flow sensors and oxygen sensors will be powered on.
3. The oxygen sensor was powered on and allowed to warm. The warm-up time includes self-calibration to air. The supporting software for the oxygen sensor displays calibration and warm-up time. The sensor output is checked with 100% and 92% oxygen to ensure the readings are accurate.
4. Once set for an experiment session, the calibration and checks do not need to be performed again. It is only repeated when the sensor has been turned off and on.
5. The pressurised air and restrictor will be set to only allow a supply of 2.5 Lpm at 29 psi.
6. The column under review will be filled with “fresh” adsorbent.
    a) Note: The adsorbent will come straight from the manufacturer and remain sealed/ uncontaminated up to testing to ensure the adsorbent has not been degraded.
    b) The adsorbent will be resealed in a nitrogen atmosphere when being stored as per the suppliers’ recommendations.

c) When tests are conducted back-to-back. Helium will be passed through the column to purge the adsorbent and clean it of any contaminant. The helium will be passed through the column at a rate of 0.25 Lpm for three minutes.

7. The timings for the solenoid valves were set in the Arduino code according to what was determined by Minitab.
8. All equipment has been prepared to start an experiment. The mass flow sensors and oxygen sensors are set to “recording” in their associated software.
9. The valve to the airline is opened. It remains open until the oxygen purity has peaked and returned to its starting air value. When this happens, the valve is closed.
10. The mass flow sensors and oxygen sensor recordings are stopped.
11. The experiment has finished.
12. Steps 3 through to 11 are repeated until all Minitab experiments are completed.

3.3. Breakthrough

The purpose of this experiment is to explore the effects of different column lengths and product flows on producing oxygen.

3.3.1. Apparatus

- Pressurised Air
- ZeoChem Samples Zeox Z12-49 (Zurich 8630, Switzerland)
- Calibrated Alicat 0-10 Lpm mass flow meter (Tucson, AZ, US)
- Calibrated Alicat 100 SCCM mass flow meter (Tucson, AZ, US)
- Restrictor – IMI Norgren T1000C1800 B7227 (Hollingworth UK)
- Swagelok needle valve x2 – SS-1RS6MM
- SST Sensing Oxygen Sesnor part number O2S-FR-T5 5 (Coatbridge, UK, ML5 4NS)
- Ardunio Uno board and 8 Channel Relay Module (Somerville, Massachusetts, US)
- Computer running:
    - Minitab (Coventry, UK)
    - Oxygen Sensor Software by SST Sensing (Coatbridge, UK, ML5 4NS)
    - Arudino Cloud Software, (Somerville, Massachusetts, US)

- Alicat logging system. Propriety software written in Python by GCE (Haydock, UK)

3.3.2. Apparatus Layout

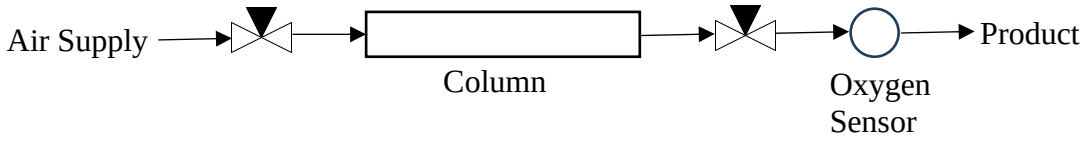

Figure 8: Breakthrough Testing Schematic Layout

3.3.3. Process

Multiple column lengths: 100 mm, 110 mm, 120 mm, 130 mm, 140 mm, 150 mm, and 160 mm, will have air passed through them at the same pressure and flow: 29 psi and 2.5 Lpm. The product flows (output from the columns) will be varied according to 20 sccm, 25 sccm, 30 sccm, 50 sccm, 75 sccm, and 100 sccm. The oxygen purity in the product flow will be recorded.

A step-step process for the experiment is as follows:

1. The equipment will be connected as per layout in
2. Figure 8. The mass flow sensors and oxygen sensors will be powered on.
3. The oxygen sensor was powered on and allowed to warm. The warm-up time includes self-calibration to air. The supporting software for the oxygen sensor displays calibration and warm-up time. The sensor output is checked with 100% and 92% oxygen to ensure the readings are accurate.
    a) Once set for an experiment session, the calibration and checks to do need to be performed again. It is only repeated when the sensor has been turned off and on.
4. The pressurised air and restrictor will be set to only allow a supply of 2.5 Lpm at 29 psi.
5. The column length under review will be filled with “fresh” adsorbent.
    a) Note: The adsorbent will come straight from the manufacturer and remain sealed/ uncontaminated up to testing to ensure the adsorbent has not been degraded.
        i) The adsorbent will be resealed in a Nitrogen atmosphere when being stored as per the suppliers’ recommendations.
    b) When tests are conducted back-to-back. Helium will be passed through the column to purge the adsorbent and clean it of any containment. The helium will be passed through the column at a rate of 0.25 Lpm for three minutes.

6. The product valve will be set to allow one of the flow values: 20 sccm, 25 sccm, 30 sccm, 50 sccm, 75 sccm, and 100 sccm.
7. All equipment has been prepared to start an experiment. The mass flow sensors and oxygen sensors are set to "recording" in their associated software.
8. The valve to the airline is opened. It remains open until the oxygen purity has peaked and returned to its starting air value. When this happens, the valve is closed.
9. The mass flow sensors and oxygen sensor recordings are stopped.
10. The experiment has finished.
11. The equipment is then prepared to perform another experiment. To do this, steps 3 to 8 are repeated. The experiment is repeated till all column lengths and flows have been tested.

3.4. Crush Testing

The purpose of this experiment is to understand the bulk crush strength of adsorbent Zeox Z12-49.

3.4.1. Apparatus

- Load Cell Instron 5987 (Wycombe, UK)
- Cylindrical holder and Piston with internal diameters 63 mm, 42 mm, 22 mm. Please see drawings in appendix D
- ZeoChem Samples Zeox Z12-49 (Zurich 8630, Switzerland)
- Scientific Sieve – Titan 10 x 450 mm mesh size 0.5 mm (Shanghai, China)

3.4.2. Process

A sample of the adsorbent will be placed in a cylindrical holder which fits with a piston. The piston will compress the adsorbent at a known weight. The sample will be sieved to determine the percentage of fines generated at that loading. The same test will be carried out across different diameters to collect enough data to determine a theory on bulk crush strength of the lithium Zeolite Z12-49 supplied by ZeoChem.

The following step-by-step procedure was created with reference to ASTM D7084-04 to guide the experimental process:

1. A fixed weight of adsorbent will be loaded into one of the three cylindrical holders: 22 mm, 42 mm, and 62 mm in diameter.
    a) Note: The adsorbent will come straight from the manufacturer and remain sealed/ uncontaminated up to testing to ensure the adsorbent has not been degraded by moisture.
2. Tap the cylindrical holder while filling to level the adsorbent in the holder. When finished gently place the piston on top of the adsorbent.
3. Load the cylindrical holder and piston into the Instron.
4. Apply one of the following loads: 10 kf-g, 20 kg-f, 30 kg-f, 40 kg-f, and 50 kg-f.
5. Remove the cylindrical holder and piston from the Instron Gently brush all the particles from the end of the piston into the scientific sieve. Pour the contents of the cylindrical holder into the scientific sieve.
6. After sieving for 60s into a weight pan, weigh the fines and the adsorbent.
7. The above steps will be repeated for each of the holders and weights to complete Table 5.

Table 5: Weight of Fines Table To be Completed

	Weight of Fines		
	Test No.		
Load (kg-f)	**1**	**2**	**3**
10			
20			
30			
40			
50			

3.5. Thermogravimetric Analysis

The purpose of the thermogravimetric analysis (TGA) was to determine if the Isotherm provided by Zeochem for their adsorbent Zeox Z12-49 was accurate for nitrogen loading.

3.5.1. Apparatus

- ZeoChem Samples Zeox Z12-49 (Zurich 8630, Switzerland)
- Crucible pans

- Mettler Toledo Thermal Analysis System TGA 2 (Columbus, Ohio)
- Nitrogen

3.5.2. Process

The TGA uses the process of heat to remove any contaminants, e.g. water, nitrogen, carbon dioxide, to produce a *"clean"* adsorbent. The temperature is then reduced and nitrogen is then introduced and the recorded weight difference is the loading of nitrogen on the adsorbent.

The following step-by-step procedure was created to guide the experimental process and ensure repeatability:

1. Using the TGA software. Create a program that determines the cycle to be performed by the TGA:
    a) For this test, the adsorbent will go through the following:
        i. Nitrogen to be supplied throughout all temperature cycles at a constant of 50mL/min.
        ii. First temperature cycle to 300ºC for 180 minutes.
        iii. Temperature to reduce to 50ºC at 10ºC a minute.
        iv. When 50ºC is achieved. Maintain for 60 minutes.
        v. Temperature to reduce to 25ºC at 10ºC a minute.
        vi. When 25ºC is achieved. Maintain for 60 minutes.
        vii. The temperature to increase to 300ºC at 2ºC a minute.
        viii. When 300 ºC is achieved, cycle ends.
2. A crucible pan is loaded with Zeochem adsorbent.
    a) Note: The adsorbent will come straight from the manufacturer and remain sealed/ uncontaminated up to testing to ensure the adsorbent has not been degraded.
3. Load the crucible into the TGA
4. Start the program
5. Return at end of program to review adsorbent weight changes.

4. RESULTS AND DISCUSSION

4.1. Aims of the Experimental Work

The aim of the experimental work are to answer the research question detailed in Section 3.3:

'Can using the RPSA cycle significantly improve oxygen yield per unit volume of adsorbent allowing the development of a small, light POC?'

To achieve this, a preliminary experiment was conducted to explore RPSA methodologies which is detailed in Section 6.2. To comprehend the results of the preliminary study, breakthrough experiments were conducted in Section 6.3. The results of the breakthrough testing were utilised in experiments to develop a novel RPSA cycle in Section 4.4.

Ancillary experiments to support the RPSA cycle development were carried out. In Section 4.6, thermogravimetric experiments were performed to understand the Nitrogen loading of Zeox Z12-49 and the literature produced by its manufacturer ZeoChem. Finally, crush test experiments were performed on Zeox Z12-49.

4.2. RPSA Methodologies

As discussed in the literature review, a few papers explored RPSA cycles but all were either too large or using pressures and flows that exceed what is possible for a portable oxygen concentrator. One paper by, Chai (2011), introduced the concept of an RPSA cycle using a small volume of adsorbent with pressures achievable with a portable oxygen concentrator.

The aim of this experiment was to replicate the Chai (2011) research to understand:

- The proposed RPSA cycle
- Why no further research was performed at these regions of pressure and flow
- Why the suggested direction of the research is to increase flow and pressure to create a "snap-on" medical oxygen concentrator.

The experiments were performed as outlined in Section 3.2. The following deviations from the Chai paper are noted:

- Chai used 90% oxygen as purge gas.
- Chai has a fixed adsorbent size of either 350 microns or 400 microns. Whereas the purchased adsorbent from Zeochem comes in a range of 400 microns to 600 microns.

The paper outlined most of the parameters for the experiment but failed to elaborate on some of the key parameters. Chai outlines the cycle as:

1. Adsorber pressurisation to a super ambient with air feed
    a) Pressure outlined in the paper as 2, 3, and 4 atmospheres. Time for this step is not provided.
2. Flow of compressed air at Pa to produce ~90% oxygen product.
    a) Output flow of the product is not provided in the paper.
3. Counter-current depressurization of column to ambient pressure level and rejection of the waste gas
    a) Time provided as 0.1 seconds.
4. Counter-current back purge of the column with a synthetic oxygen product gas at near ambient pressure and rejection of the effluent gas.
    a) Time provided as 1.4 seconds. The pressure and flow rate of oxygen is not provided.
5. Repeat

The overall cycle time for the experiments was between 2.5 seconds to 5.5 seconds with 5.5 seconds providing the best results. This leaves time for steps 1. and 2. as unknown. The input and output flow are not provided in the paper. The following assumptions can be made for the flows:

- Output – in the conclusion of the paper proposal is given for a device which can achieve 15.8 Lpm output for 230 g which suggests an efficiency 0.068 Lpm per gram. With a suggested weight of 1 gram for the experimental set-up. This would suggest an output of 0.068 Lpm can be achieved with the experiment.
- Input – this will have to be judged. As the aim of this paper is to achieve an RPSA cycle which can be used in a POC. The input flow will be set to 12 Lpm.

Using the methodology outlined in Section 6.2 with the above information extracted from the Chai paper, the test results per Figure 9 were obtained.

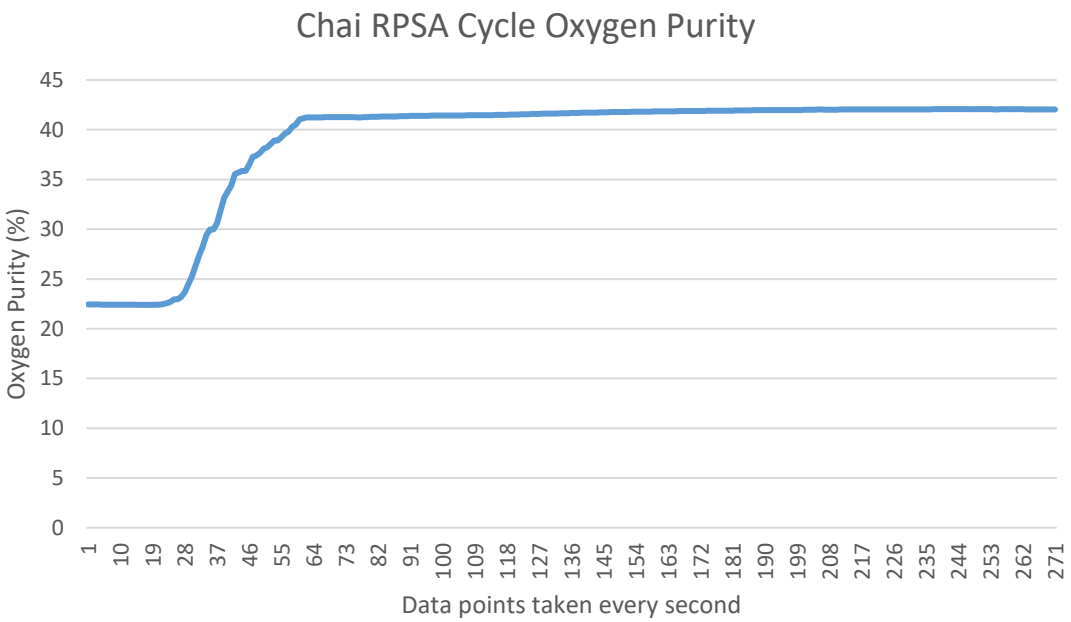

Figure 9: Repeat of Chai (2011) Experimental Results

Multiple tests were run varying the unknown factors to improve the product purity and match the results of the paper. Regardless of how the system was configured the purity only reached 56%, per Figure 10 .

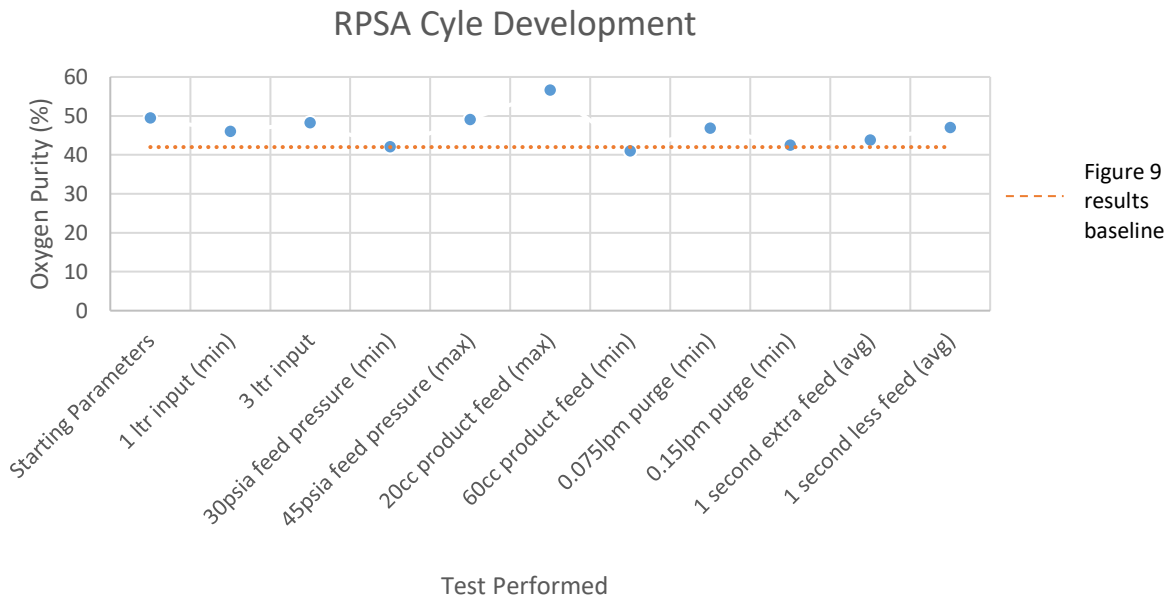

Figure 10: Chai Experiment Cycle Development Results

4.2.1. RPSA Methodologies Results Discussion

The result from the Chai RPSA experiments did not yield the same outcome as the original paper. The oxygen yield was unexpectedly significantly lower. This is attributed to a few factors in the experiment. The use of 90% oxygen as a purge gas will artificially inflate what

can be achieved with the RPSA cycle. To prove this theory, a test will be performed using the methodology outlined in Section 5.2 and the RPSA cycle that yielded the best results. When steady state has been achieved. The 90% oxygen purge will be introduced to highlight its impact. The results of the test are shown in Figure 11 and are broken down into three sections.

- Per Figure 11, section A shows the results of the RPSA running at its top performance
- Per Figure 11, section B is a drop in purity which comes from the pressure dropping as the purge gas is switched to the 90% oxygen
- Per Figure 11, section C reflects the effect of 90% oxygen being added to the RPSA cycle. It can clearly be seen that with no changes to the cycle using 90% oxygen artificially inflates the product purity.

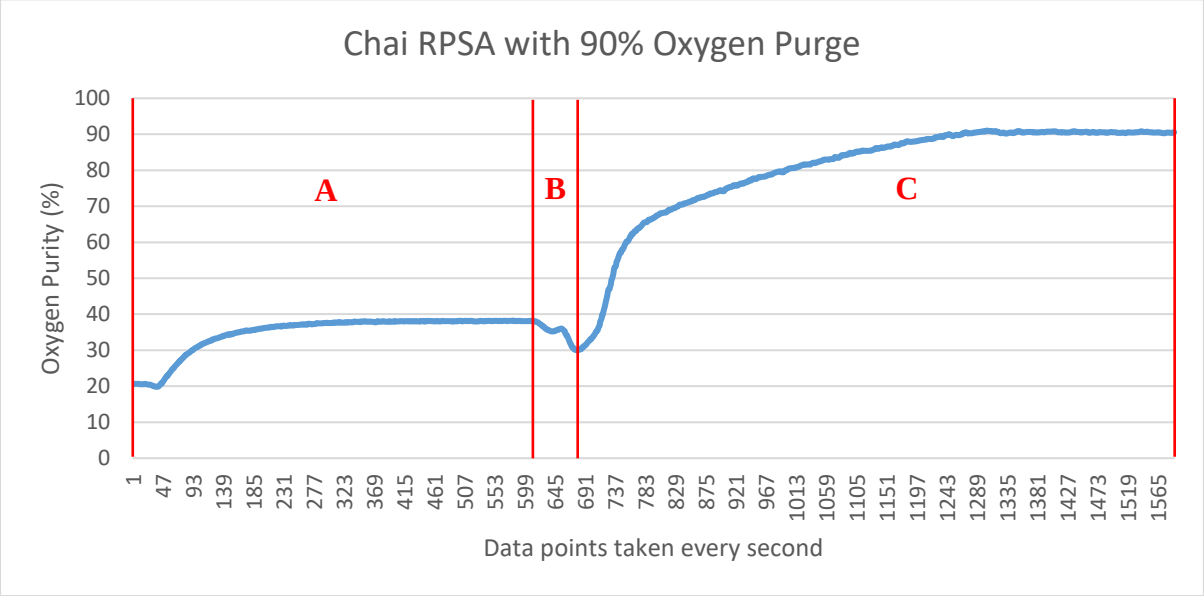

Figure 11: Chai Experiment With 90% Oxygen Purge Added During Test

Another factor to consider is that the length of the column being proposed is not ideal. As explored in Section 4.4 of the literature review, the smaller columns and higher gas throughputs of a RPSA system result in higher pressure drop leading to an increase in interstitial velocity. This can lead to early breakthrough of concentration Sundaram (1988), Kikkinides (1993) and Yang (1998).

This theory can only be fully explored and understood by performing breakthrough tests. This will be explored and discussed further in Section 6.3.

4.3. Breakthrough

The unexpected results of the experiment performed in Section 4.2 will be better understood by performing breakthrough tests on a range of column lengths from 100 mm to 160 mm. To better understand column dynamics and determine the best column length. As such, a series of breakthrough tests will be performed according to the equipment and methodologies outlined in Section 3.3. The results of the breakthrough tests are shown in Table 6 and Figure 12.

Table 6: Oxygen Purity (%) Results for Varying Column Lengths and Product Flows

Product Flow (sccm)	Column Length (mm)						
	100	**110**	**120**	**130**	**140**	**150**	**160**
20	65.9%	69.6%	75.2%	75.1%	80.4%	82.2%	82.3%
25	66.7%	73.0%	76.7%	78.4%	81.4%	81.9%	83.6%
30	64.5%	75.2%	77.1%	79.2%	82.1%	83.2%	86.0%
50	65.7%	73.4%	75.6%	82.8%	85.6%	85.3%	83.6%
75	63.4%	70.0%	75.6%	80.8%	81.8%	83.4%	82.3%
100	60.4%	65.8%	68.1%	72.6%	76.7%	74.4%	82.3%

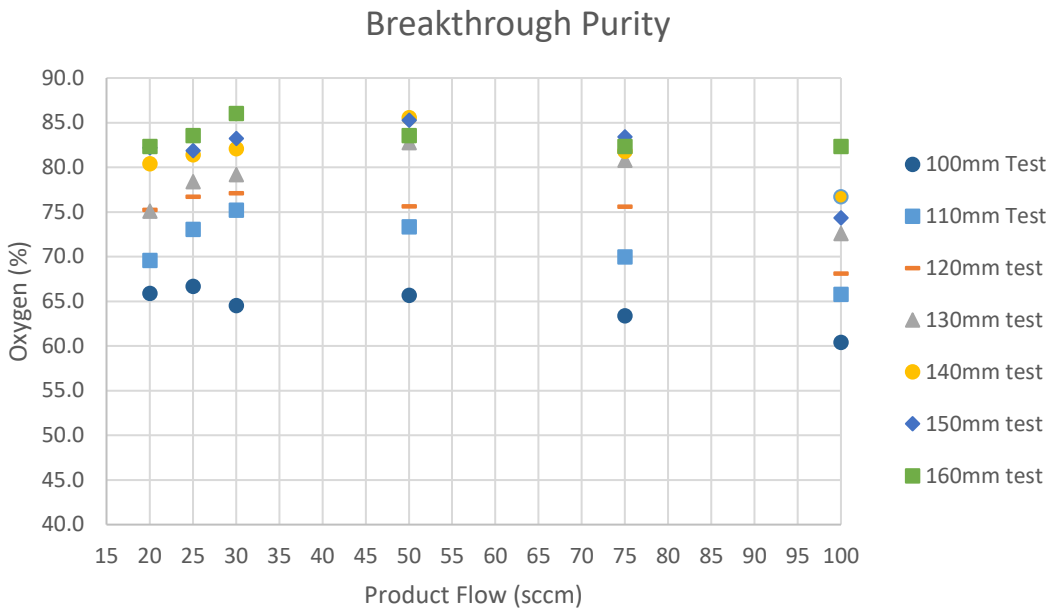

Figure 12: Table 6 Breakthrough Purity Results Plotted On A Scatter Graph

4.3.1. Breakthrough Results and Discussion

Important conclusions can be drawn from the results.

The 110 mm column proposed by the Chai (2011) paper and used in the Section 6.2 experiments was not ideal. The highest purity that could be achieved was 75.2% with a lower product flow than proposed in the Chai paper. The 110 mm column is experiencing the early breakthrough due to its short length and high interstitial velocities created by the high pressure drop from the use of small beads.

The theory that the smaller beads are having a negative impact on the breakthrough can be tested further. One of the noted test exceptions from the Chai experiments was the use of smaller beads, 350 microns or 400 micro, in the paper. Whereas Adsorbent Zeox Z12-49 is purchased from Zeochem with a bead size of 400-600 microns. To understand the impact of using smaller adsorbents, the Zeox Z12-49 was sieved to collect beads smaller than 500 microns. Using the 140 mm column, the breakthrough testing will be reperformed on the smaller beads in accordance with the methodologies outlined in section 3.3.

The results of the smaller bead breakthrough testing is shown in Table 7. The smaller beads produced a lower purity product than the commercially purchased Zeox Z12-49. The lower results can be attributed to the same effect seen with using the 110 mm column. The smaller

beads will increase the pressure drop across the column and will in turn increase interstitial velocities within the bed leading to early breakthrough.

Table 7: Small Bead Breakthrough Comparison

Product Flow (sccm)	Column Length and Bead Size	
	140 mm Test Commercial Bead	**140 mm Test < 500 µm Bead**
20	80.4%	77.27%
25	81.41%	79.15%
30	82.07%	80.72%
50	85.56%	80.93%
75	81.8%	79.25%
100	76.7%	75.99%

The results of the breakthrough experiments paired with the test using 90% oxygen has helped invalidate the results of the Chai 2011 paper and validate the results of Section 6.2.

The breakthrough experiments have helped determine a column length which should be more Suitable for use with the proposed Chai RPSA cycle. At the lower flows with each increasing column length the product purity increases but as the product flow increases the purity begins to drop. This is to be expected with the interstitial velocities theory. The captivating result from the breakthrough experiments in the grouping of the results for the 140 mm, 150 mm, and 160 mm columns which yield the highest product purities. This indicates that with a diameter of 4 mm, as suggested by the Chai paper, regardless of increasing the length of the column, the product output will remain nearly the same. This would suggest that increasing the column length will not improve the output and that there is a limit to the useful length of the column.

If the 140 mm, 150 mm, and 160 mm columns yield similar results. The 140 mm column will be used to improve the results from the experiments in Section 4.2 and to develop a new RPSA cycle. The aim of this research is to determine if an RPSA cycle can be used to develop a small, light POC. By using the 140 mm column there is a 0.28 g weight saving overusing the 160 mm column.

To determine the accuracy of the results in Table 6 and Figure 12. The experiment was repeated multiple times for the 130 mm, 140 mm, and 150 mm columns at a flow of 50 sccm. The outcome of the repeated testing is shown in Table 8 and Figure 13. The results fell within one standard deviation. This means the experiment is repeatable and the results from the breakthrough testing are reliable. The same reliability can be extended to the RPSA testing as the experimental processes are like the breakthrough experiments.

Table 8: Breakthrough Repeatability Review

	130 mm, 50 sccm	**140 mm, 50 sccm**	**150 mm, 50 sccm**
	81.7%	84.32%	83.89%
	82.75%	84.38%	84.72%
	82.93%	85.56%	85.28%
STDEV	0.66	0.69	0.69
MEAN	82.46%	84.75%	84.63%

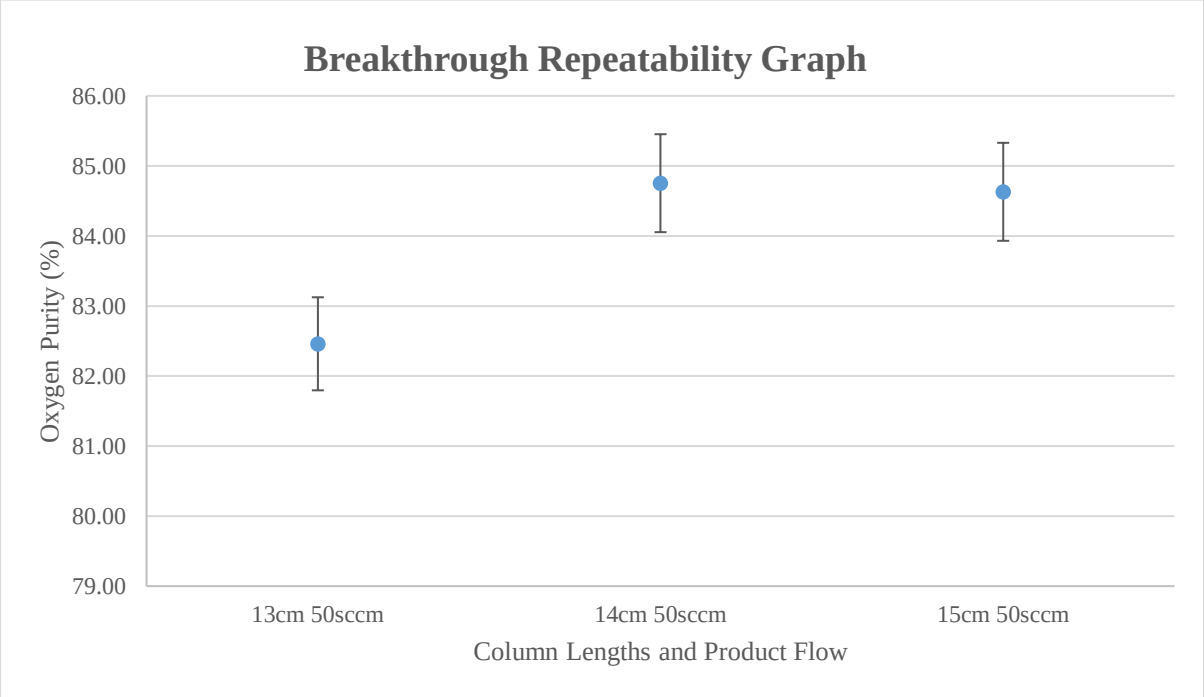

Figure 13: Breakthrough Repeatability Graph

In conclusion, the results of the breakthrough tests have confirmed the poor results of the experiments performed in Section 6.2. It has also helped determine a column length that could result in improved product purity if used with the Section 6.2 experiments.

4.4. RPSA Development

The breakthrough testing identified that a 140 mm column will yield improved product purity from the experiments performed in Section 6.2. Using the methodology outlined in Section 5.2 and the timings from the best results in Section 6.2. The 140 mm column will be tested.

With a direct comparison to the 110 mm column and no other changes to the cycle. The 140 mm column improved the product purity, as shown in Figure 14.

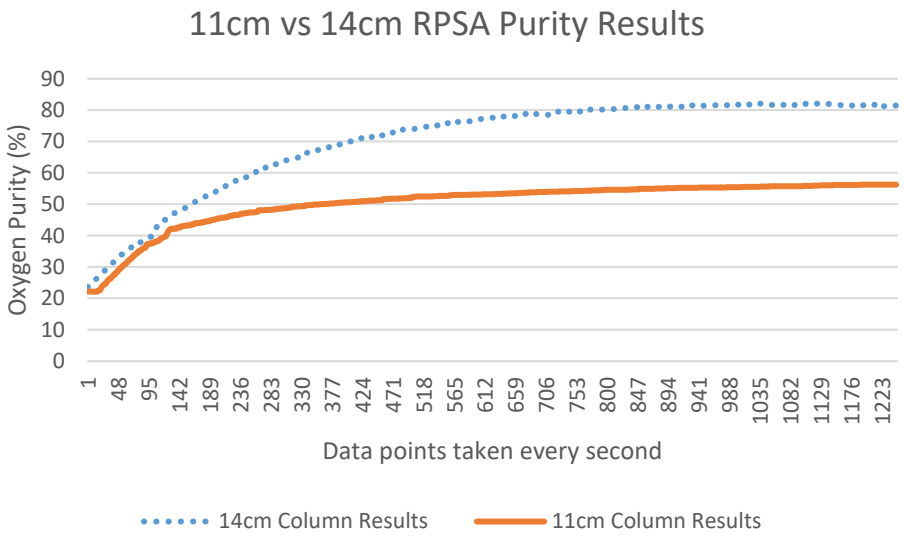

Figure 14: RPSA 100 mm Column Results Compared with 140 mm Column Results

The results with the longer column are improved but are still lower than the reported results that could be achieved by the Chai 2011 paper.

The next step in developing an RPSA is to maintain the suggested experimental layout from the Chai paper as this is relatively common in academic literature but to move away from the suggested timings and pressures of the paper to develop a novel cycle.

To do this, a statistical Design of Experiments (DoE) technique will be used. A DoE will allow all the different parameters: timings, flow, and pressures to be explored and their impact and relationships understood to develop the cycle.

Using the software package Minitab. A first order DoE will be used to optimise the variable parameters of the RPSA cycle. An initial 2^k factorial DoE model will be tested. The assumption when using 2^k factorial models is that the variable parameters being screened typically follow a linear trend. If the variables are non-linear and show some curvature. The

first order model is inadequate, and a second order model will be needed. To test curvature, centre points can be added to the 2^k factorial model.

In the RPSA cycle there are the following parameters: input flow, input pressure, product valve time, product flow, feed valve time, purge valve time, product refill time, and purge flow. Using a 2^k factorial model with centre points in Minitab this would create 264 tests to be conducted. As outlined in the methodologies, tests will have to run for 20 minutes to reach a steady state which is just under 90 hours of testing. To streamline the testing, the number of parameters for the DoE can be reduced by considering:

- Input flow will be set to 2.5 Lpm but is limited to the valve timings
- Pressure will be set to 28.5 psi which is an achievable pressure from a POC compressor
- Product valve time is a factor of the purge and delay time. The product valve time will be altered by modifying the other parameters.
- Product flow will be fixed to 50 sccm.

The remaining parameters to be considered by the DoE are: feed valve time, purge valve time, product refill time, and purge flow. This reduces the parameters to be considered down to 4. This results in the number of tests being reduced to 16. By including centre points, the total number of tests is 17.

The starting centre-points and limits of the identified parameters are outlined in Table 9 and have been guided by the experimental work conducted in Section 6.2. The chosen values are a starting point and can be adjusted depending on the results of the DoE.

Table 9: 2^k Factorial DOE Parameters

	Lower Limit	**Centre Point**	**Upper Limit**
Feed valve time (s)	1.5	2.00	2.5
Purge Valve time (s)	1	1.250	1.5
Product Refill time (s)	0.15	0.25	0.35
Purge Flow (Lpm)	0.140	0.150	0.160

With the parameters defined and using the methodology outlined in section 3.2 a working novel RPSA cycle can be developed. To start, the variable parameters will be input into Minitab. This will determine the 18 tests to be conducted, Table 10 outlines the list of experiments.

Table 10: DOE 2k Factorial Determined Experiments

Test Run No.	Purge Flow (Lpm)	Feed Valve Time (s)	Purge Valve Time (s)	Product Refill Time (s)
1	0.13	1	0.75	0.05
2	0.17	1	0.75	0.05
3	0.13	3	0.75	0.05
4	0.17	3	0.75	0.05
5	0.13	1	1.75	0.05
6	0.17	1	1.75	0.05
7	0.13	3	1.75	0.05
8	0.17	3	1.75	0.05
9	0.13	1	0.75	0.45
10	0.17	1	0.75	0.45
11	0.13	3	0.75	0.45
12	0.17	3	0.75	0.45
13	0.13	1	1.75	0.45
14	0.17	1	1.75	0.45
15	0.13	3	1.75	0.45
16	0.17	3	1.75	0.45
17	0.15	2	1.25	0.25

Each test was performed recording the input flow, input pressure, output flow, output pressure, purge flow, purge pressure, and product purity. Only the product purity will be added to Minitab to determine the optimum variables for the RPSA. All 17 experiments were conducted, per Table 11.

Table 11: DOE 2k Factorial Experimental Collected Data

Test Run No.	Purge Flow (Lpm)	Feed Valve Time (s)	Purge Valve Time (s)	Product Refill Time (s)	Purity (%)
1	0.13	1	0.75	0.05	84.21
2	0.17	1	0.75	0.05	83.26
3	0.13	3	0.75	0.05	83.99
4	0.17	3	0.75	0.05	84.84
5	0.13	1	1.75	0.05	82.39
6	0.17	1	1.75	0.05	84.66
7	0.13	3	1.75	0.05	84.34
8	0.17	3	1.75	0.05	86.16
9	0.13	1	0.75	0.45	81.23
10	0.17	1	0.75	0.45	85.56
11	0.13	3	0.75	0.45	83.25
12	0.17	3	0.75	0.45	83.89
13	0.13	1	1.75	0.45	81.17
14	0.17	1	1.75	0.45	83.93
15	0.13	3	1.75	0.45	83.06
16	0.17	3	1.75	0.45	85.65
17	0.15	2	1.25	0.25	85.4

From the results in Table 12 and Figure 15 it can be determined that the 2^k factorial model for a design of experiments model is not reliable. The centre points are so far off the expected trajectory of the model, Minitab is unable to determine a calculation to optimise the design. This is why in Table 12 there is no results for p-values determined by Minitab as there is insufficient degrees of freedom to calculate.

Table 12: Minitab 2k Factorial Results

Term	Effect	Coef	SE Coef	T-Value	P-Value	VIF
Constant		83.85	*	*	*	
Purge Flow	1.7888	0.8944	*	*	*	1
Feed Valve Time	1.0962	0.5481	*	*	*	1
Purge Valve Time	0.14125	0.07063	*	*	*	1
Product Refill Time	-0.7637	-0.3819	*	*	*	1
Purge Flow*Feed Valve Time	-0.3138	-0.1569	*	*	*	1
Purge Flow*Purge Valve Time	0.5712	0.2856	*	*	*	1
Purge Flow*Product Refill Time	0.7913	0.3956	*	*	*	1
Feed Valve Time*Purge Valve Time	0.6688	0.3344	*	*	*	1
Feed Valve Time*Product Refill Time	-0.10625	-0.05313	*	*	*	1
Purge Valve Time*Product Refill Time	-0.17125	-0.08562	*	*	*	1
Purge Flow*Feed Valve Time*Purge Valve Time	0.15875	0.07937	*	*	*	1
Purge Flow*Feed Valve Time*Product Refill Time	-0.6512	-0.3256	*	*	*	1
Purge Flow*Purge Valve Time*Product Refill Time	-0.4762	-0.2381	*	*	*	1
Feed Valve Time*Purge Valve Time*Product Refill Time	0.14625	0.07313	*	*	*	1
Purge Flow*Feed Valve Time*Purge Valve Time*Product Refill Time	0.7212	0.3606	*	*	*	1
Ct Pt		1.551	*	*	*	1

It can be seen from the main effect plots per Figure 15, that the variable parameters are non-linear as the centre point data does not sit on the line.

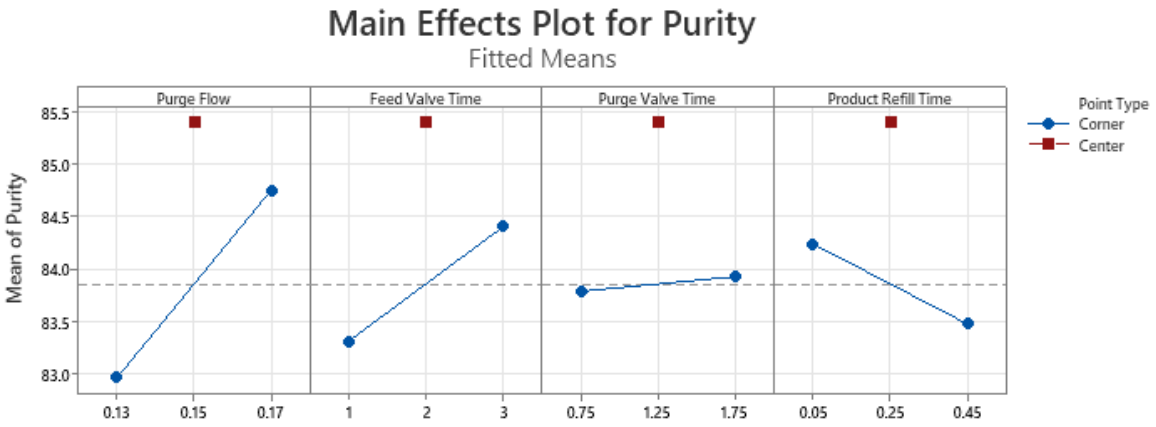

Figure 15: DOE 2k Factorial Main Effects

The next DoE study will be performed using RSD (Response Surface Design). This is a more advanced DoE and is capable of monitoring curvature and 2nd order quadratic relationships. The RSD will be performed under a Central Composite Design (CCD), the curvature is determined by the centre points and the quadratic terms are determined by axial points. The CCD increases the number of tests for the quadratic level and takes the DoE study up to 31 tests, as shown in Table 13. The increased number of tests performed when compared with a 2^k factorial model may increase the complexity but will improve the reliability of the results.

Table 13: DOE RSD Experiment List

Test Run No.	Purge Flow (Lpm)	Feed Valve Time (sec)	Purge Valve Time (sec)	Product Refill Time (sec)
1	0.14	1.5	1	0.15
2	0.16	1.5	1	0.15
3	0.14	2.5	1	0.15
4	0.16	2.5	1	0.15
5	0.14	1.5	1.5	0.15
6	0.16	1.5	1.5	0.15
7	0.14	2.5	1.5	0.15
8	0.16	2.5	1.5	0.15
9	0.14	1.5	1	0.35
10	0.16	1.5	1	0.35
11	0.14	2.5	1	0.35
12	0.16	2.5	1	0.35
13	0.14	1.5	1.5	0.35
14	0.16	1.5	1.5	0.35
15	0.14	2.5	1.5	0.35
16	0.16	2.5	1.5	0.35
17	0.13	2	1.25	0.25
18	0.17	2	1.25	0.25
19	0.15	1	1.25	0.25
20	0.15	3	1.25	0.25
21	0.15	2	0.75	0.25
22	0.15	2	1.75	0.25
23	0.15	2	1.25	0.05
24	0.15	2	1.25	0.45
25	0.15	2	1.25	0.25
26	0.15	2	1.25	0.25
27	0.15	2	1.25	0.25
28	0.15	2	1.25	0.25
29	0.15	2	1.25	0.25
30	0.15	2	1.25	0.25
31	0.15	2	1.25	0.25

The new list of tests, per Table 13, were performed using the methodology outlined in Section 3.2 As per the previous tests, the input flow, input pressure, output flow, output pressure, purge flow, purge pressure, and product purity, were recorded. The product purity will be input into Minitab, per Table 14, for it to determine the best parameters for the RPSA.

Table 14: DOE RSD Experiment Collected Data

Test Run No.	Purge Flow (Lpm)	Feed Valve Time (sec)	Purge Valve Time (sec)	Product Refill Time (sec)	Purity (%)
1	0.14	1.5	1	0.15	84.21
2	0.16	1.5	1	0.15	83.26
3	0.14	2.5	1	0.15	83.99
4	0.16	2.5	1	0.15	84.84
5	0.14	1.5	1.5	0.15	82.39
6	0.16	1.5	1.5	0.15	84.66
7	0.14	2.5	1.5	0.15	84.34
8	0.16	2.5	1.5	0.15	86.16
9	0.14	1.5	1	0.35	81.23
10	0.16	1.5	1	0.35	85.56
11	0.14	2.5	1	0.35	83.25
12	0.16	2.5	1	0.35	83.89
13	0.14	1.5	1.5	0.35	81.17
14	0.16	1.5	1.5	0.35	83.93
15	0.14	2.5	1.5	0.35	83.06
16	0.16	2.5	1.5	0.35	85.65
17	0.13	2	1.25	0.25	84.31
18	0.17	2	1.25	0.25	85.08
19	0.15	1	1.25	0.25	71.96
20	0.15	3	1.25	0.25	86.83
21	0.15	2	0.75	0.25	85.83
22	0.15	2	1.75	0.25	84.62
23	0.15	2	1.25	0.05	87.09
24	0.15	2	1.25	0.45	84.08
25	0.15	2	1.25	0.25	85.4
26	0.15	2	1.25	0.25	86.1
27	0.15	2	1.25	0.25	85.6
28	0.15	2	1.25	0.25	84.9

Table 14: DOE RSD Experiment Collected Data (Continued)

Test Run No.	Purge Flow (Lpm)	Feed Valve Time (sec)	Purge Valve Time (sec)	Product Refill Time (sec)	Purity (%)
29	0.15	2	1.25	0.25	84.3
30	0.15	2	1.25	0.25	84.8
31	0.15	2	1.25	0.25	84

This time from the results, the curvature can be seen in Figure 15, and the trend of the results follows the normal distribution plot. We can conclude from these results that the RSD DoE is a more accurate model for calculating the best RPSA parameters. The RSD DoE has been able to determine main effects with curvature and determine a model from the data.

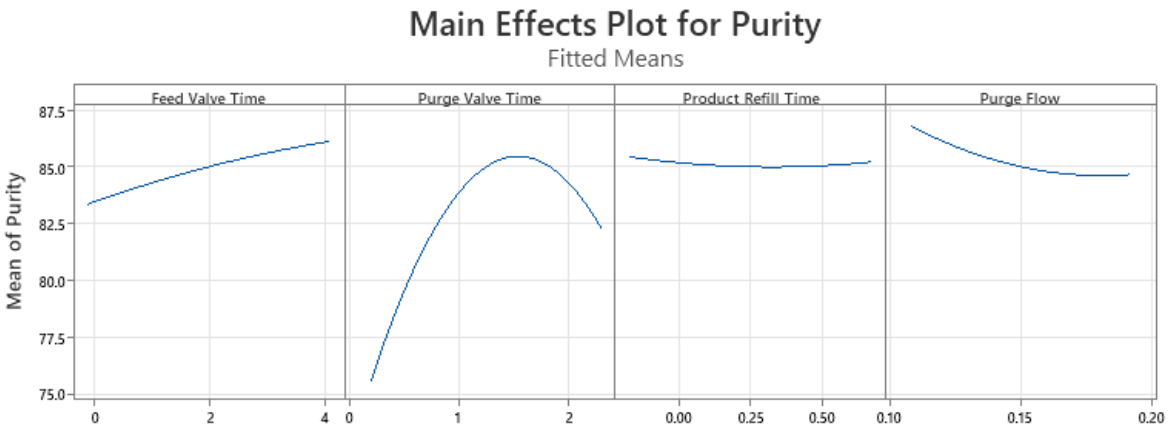

Figure 16: DOE RSD Main Effects

With an accurate model, the DoE results can be analysed further. Minitab generated a pareto chart ranking the parameters against their impact on the RPSA system, Figure 17. The pareto chart shows a line of statistical significance at 2.120 and the factors that surpass the line are statistically significant. In this DoE, parameter B:Feed Valve Time represents the most influential factor to RPSA time.

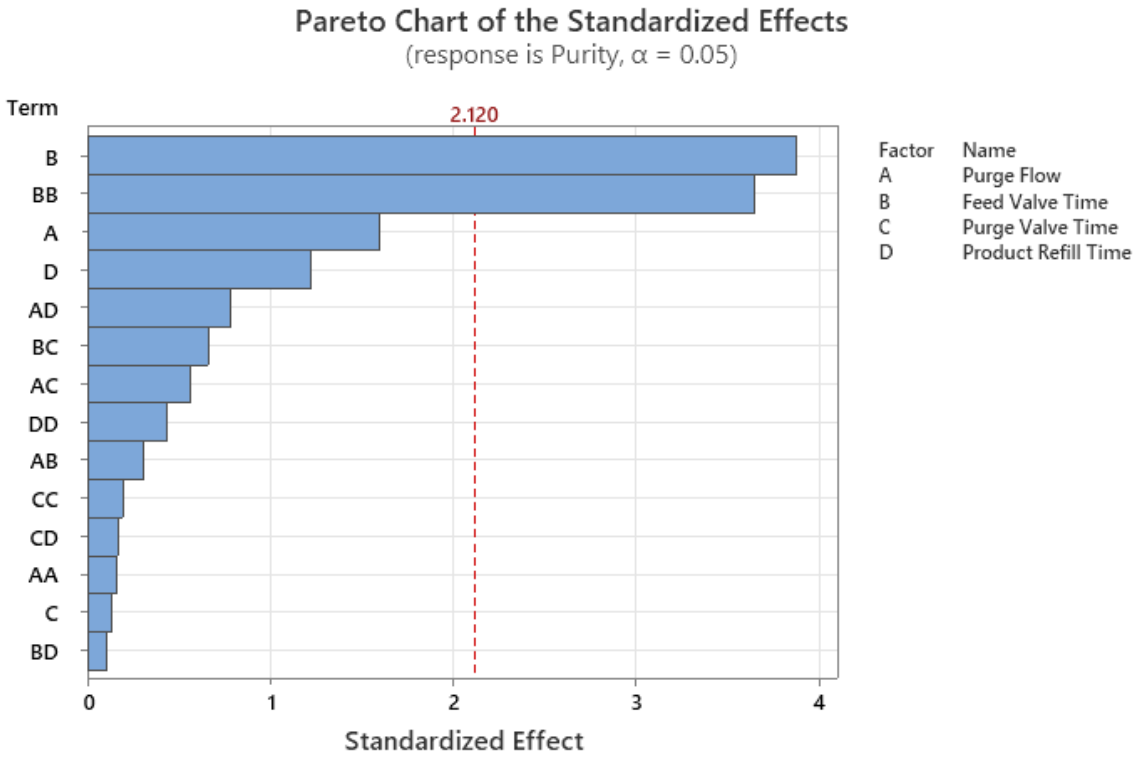

Figure 17: DOE RSD Pareto Chart

Minitab can optimise the results to determine the best parameters for generating the highest oxygen purity using a model it generated from the test results. It can be seen in Figure 18 that Minitab would recommend the following parameters to achieve a purity of 88.23%: purge flow of 0.130 Lpm; feed valve time of 2.25 s; purge valve time of 0.750 s; and finally, a product refill time of 0.050 s. Running the recommended parameters by Minitab generated the following purity 87.43%.

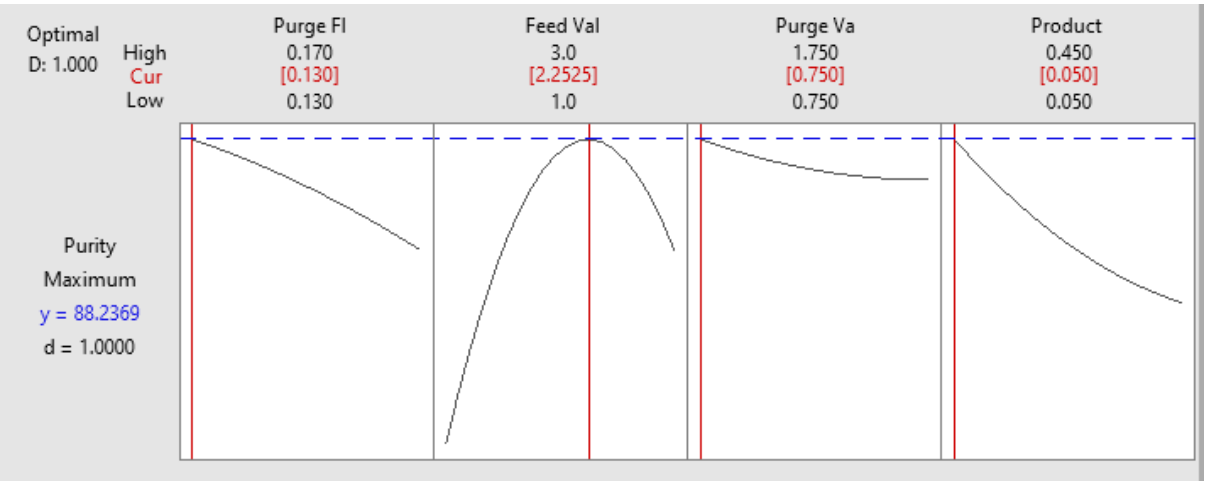

Figure 18: DOE Optimized Results

4.4.1. RPSA Development Discussion and Results

The optimum parameters determined by Minitab have not yielded the expected results, which do not come as a surprise. The Minitab results only determined that the feed valve timing was significant, see Figure 17. This is further highlighted in the results of the analysis of the variance results from Minitab, see Table 15.

Table 15: DoE RSD Results

Source	DF	Adj SS	Adj MS	F-Value	P-Value
Model	14	143.301	10.2358	2.49	0.042
Linear	4	78.460	19.6150	4.76	0.010
Purge Flow	1	10.468	10.4676	2.54	0.130
Feed Valve Time	1	61.793	61.7925	15.00	0.001
Purge Valve Time	1	0.069	0.0693	0.02	0.898
Product Refill Time	1	6.131	6.1307	1.49	0.240
Square	4	58.686	14.6714	3.56	0.029
Purge Flow*Purge Flow	1	0.100	0.0999	0.02	0.878
Feed Valve Time*Feed Valve Time	1	54.781	54.7812	13.30	0.002
Purge Valve Time*Purge Valve Time	1	0.154	0.1541	0.04	0.849
Product Refill Time*Product Refill Time	1	0.764	0.7636	0.19	0.673
2-Way Interaction	6	6.155	1.0258	0.25	0.953
Purge Flow*Feed Valve Time	1	0.394	0.3938	0.10	0.761
Purge Flow*Purge Valve Time	1	1.305	1.3053	0.32	0.581
Purge Flow*Product Refill Time	1	2.504	2.5043	0.61	0.447
Feed Valve Time*Purge Valve Time	1	1.789	1.7889	0.43	0.519
Feed Valve Time*Product Refill Time	1	0.045	0.0452	0.01	0.918
Purge Valve Time*Product Refill Time	1	0.117	0.1173	0.03	0.868
Error	16	65.897	4.1186		
Lack-of-Fit	10	62.629	6.2629	11.50	0.004
Pure Error	6	3.269	0.5448		
Total	30	209.198			

Feed valve is the only parameter with a p-value under 0.05 meaning its impact is significant. The other parameters and their interactions are considerably higher. The next closest parameter is purge flow with a p-value of 0.130.

The issue with the lack of fit can be attributed to the chosen range for the parameters. From Figure 18, Minitab's suggested optimised parameters are at the limits of the tested range. More time and resources should be committed to adjusting the parameters with the following considerations:

- The product refills takes the oxygen product and recycles it back through sieve to help with increasing purity. Minitab has suggested the time for this phase should be 0.050 seconds. This time cannot be reduced any further and remain useful. It suggested that the valve timing remains the same.
- The purge valve and purge flow are connected. This sequence takes the oxygen product and uses it to purge/clean the adsorbent for the next cycle. Minitab has

suggested the RPSA cycle uses the lowest flow and shortest valve time for this step. This is because, by taking the product out of the patient tank, the system pressure is reduced. Without the head of pressure in the patient tank this allows earlier breakthrough of the nitrogen in the earlier phases of the RPSA cycle. It would be suggested that for further cycle development these parameters should be widened to allow Minitab to determine the best flow and valve timing. The oxygen purge is critical for regenerating the adsorbent but too much purge drops the product purity. As such, finding the right balance is critical.

- Of the other parameters in the RPSA
  - The input flow has remained fixed at 2.5 Lpm from the initial RPSA experiments based on the Chai paper. This could be factored into the Minitab DoE but it should be noted that the input flow will impact the breakthrough. As such, a change to the input flow should be considered with further breakthrough testing to ensure the column length remains correct and early breakthrough is not happening.
  - The input pressure of 28.5 psi has been selected based off the achievable pressures for the current state of the art in portable oxygen concentrators determined from the extensive market review and industry experience.
  - The product time is a factor of the feed valve timing and purge valve timing which are both considered in the DoE. The third input to product time is a fixed delay of 0.5 seconds. The fixed delay could be considered in further DoE work and be an interesting parameter to be considered. Insufficient time and the adsorbate will not fully purge. Too long, and the system pressure will decrease to far with the constant product output of 0.5 Lpm. If the right time is found for depressurisation this may allow an increased time for purging due to the system pressure being maintained.

The results of the RPSA experimental work was 2.57% off the target of 90% product purity which is the average expected level of oxygen from a POC in the medical market. However, it should be noted that medical POC devices are design to BS EN ISO 80601-2-69:2020 and the international standard expects a minimum of 82% oxygen product before an alarm should be activated to alert users.

The important conclusion from the experimental work is that an RPSA cycle using a small column can achieve oxygen purities accepted by the POC industry standards. It is firmly believed that with further DoE work and the suggested improvements of this section higher purities will be achieved. How this system can be utilised to benefit the design of a POC will be fully explored and discussed in section 5.

4.5. Adsorbent Stress

During the extensive RPSA testing it appeared that the adsorbent was beginning to break down. This was evident from the dust that was appearing on or around the columns, see Figure 19 and Figure 20.

Figure 19: Dust Observed Inside Column Connections

Figure 20: Dust Observed Outside Column Connections

The higher gas throughputs of an RPSA system result higher in a pressure drop. This increases the axial pressure gradient until a limit is reached. When this threshold is reached

fluidization occurs resulting in rapid attrition of the particle Todd (2005). Understanding pressure drop in the column is going to be vital. Higher pressures allow great Nitrogen loading on the adsorbent but increased pressure can come at a cost to adsorbent damage and longevity. By calculating and measuring the pressure drop. A loading on the adsorbent can be determined and tested to understand the crushing effects.

As outlined in the literature review, the Ergun Equation has been used for determining pressure drops in packed columns with the following Equation:

$$-\frac{\Delta p}{L} = 150\frac{(1-\varepsilon_b)^2}{\varepsilon_b^3}\frac{\eta u_z}{d_p^2} + 1.75\frac{(1-\varepsilon_b)}{\varepsilon_b^3}\frac{\rho u_z|u_z|}{d_p} \tag{16}$$

This will be used to review pressure drop in relation to experimental data across the 100 mm, 110 mm, 120 mm, 130 mm, 140 mm, 150 mm, and 160 mm columns packed with commercially available adsorbent. The measured and theoretical results are outlined in Figure 21.

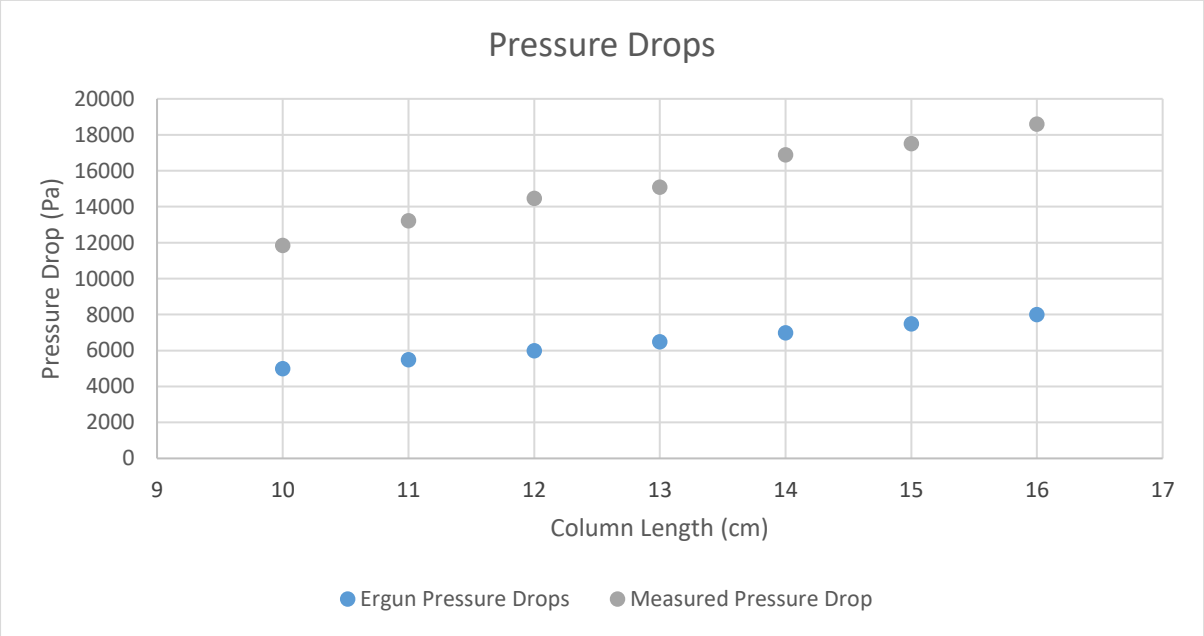

Figure 21: Ergun Equation Results Compared to Measured Pressure Drop

It is noted from the results that the calculated pressure drop is much lower than the measured. Literature from Todd (2005), Raichura (1999), and Macdonald *et al.*. (1979) reviewed pressure drop through porous media and determined that the constants can be calibrated through experiments to more accurately determine pressure drop theoretically. The constant

needing review is the ε_b – interparticle void fraction. Ergun reviewed larger particles leading to the constant of 0.37 being suggested. As such, the smaller particles being used in this RPSA system will have a lower void fraction than the original paper. By reducing the interparticle void fraction by ~20% to 0.3 the calculated and measured align, see Figure 22.

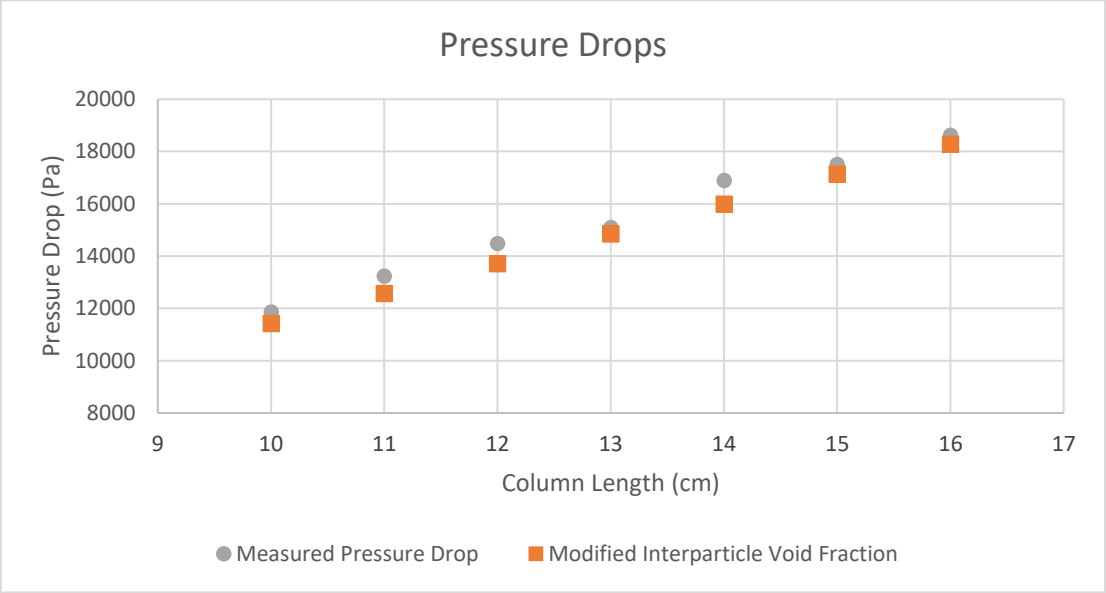

Figure 22: Modified Ergun Equation Results Compared to Measured Pressure Drop

Understanding the pressure drop in the RPSA system through experimental and theoretical methods. Will be critical when understanding how the RPSA system fits into a portable oxygen concentrator system. While measuring the pressure drop a load can be determined which has been crushing the adsorbent. The inlet pressure recorded during the pressure drop experiments was 20psi. From this, a loading on the adsorbent can be determined across the diameter of the column and further diameters to draw a correlation between load and diameter, see Table 15. This is done using:

$$F = P \; x \; A \tag{17}$$

Table 16: Calculated Load over Diameter

Column Dia (mm)	Load (kg-f)
6.8	2.03
12	6.32
22	21.26
42	77.50
64	179.97

For the experiment, multiple diameters will be tested with varying loads as outlined in Section 3.4. The results of the crush tests are outlined in Table 16 and Figure 23.

Table 17: Crush Test Weighed Fines

Load (kg-f)	Weight (mg) of fines from 63mm Dia test	Weight (mg) of fines from 42mm Dia test	Weight (mg) of fines from 22mm Dia test
10	0.01353	0.00388	0.00106
20	0.01723	0.00451	0.00159
30	0.02706	0.0109	0.00575
40	0.0317	0.01055	0.00541
50	0.0457	0.0324	0.00722

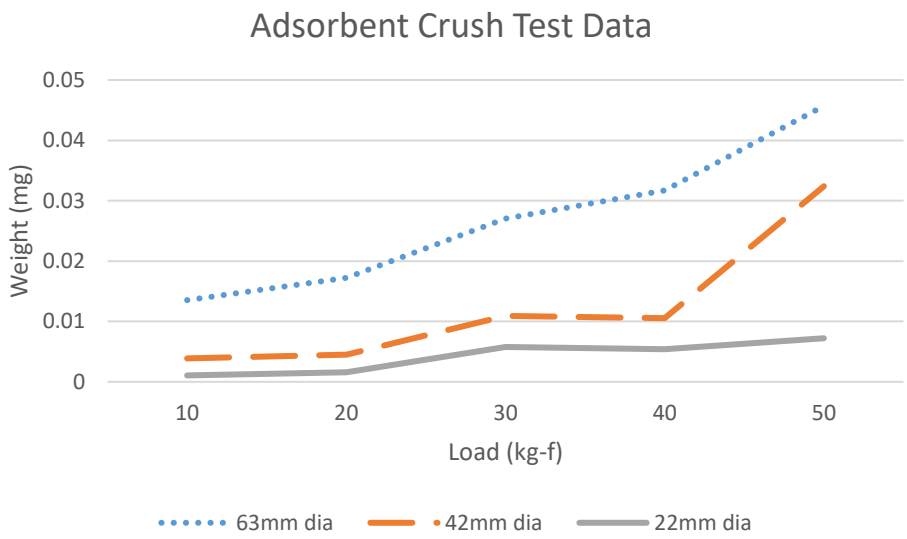

Figure 23: Plotted Crush Test Results

4.5.1. Adsorbent Stress Discussion

The results of the crush testing were not significant. As expected, the load over the larger area created a greater number of fines. Further development will be needed to understand the correlation between pressure drop and the crushing of adsorbent.

It is important to understand and limit the production of dusting in an RPSA system. The dust produced can travel downstream and break the delicate valves used in circuit. Further research in this area would be highly beneficial and should be considered for future review.

The pressure drop experimental and theoretical work yielded better results. The experimental work guided how the Ergun Equation can be modified to accurately determine pressure drop within 5% of the measured. This will be very beneficial when understanding how the RPSA system will work in a portable oxygen concentrator when determining power consumption.

4.6. Thermogravimetric Analysis

To enable further theoretical understanding of the commercially purchased adsorbent, Z12-049. It is important to review the nitrogen adsorbent loading as advertised by the supplier Zeochem in their available literature, see Figure 24, to determine if it can be relied upon for theoretical calculations and deeper understanding.

To confirm the published data from Zeochem, which can't be disclosed in this report due to the nature of the information. Thermogravimetric Analysis (TGA) experiments were performed according to the methodologies outlined in Section 3.5. The aim of the experiments was to determine the nitrogen loading at atmospheric pressure at 25 ºC and 50 ºC.

According to the data shared by Zeochem. The expected loading at atmospheric pressure is 1.1 times its base weight. The results from Figure 24 show that after purging the adsorbent sample by exposing it to 300 ºC for 180 minutes the base weight is 22.31 mg, (see 'A' per Figure 25). After being exposed to Nitrogen for 180 minutes at 25 ºC and 50 ºC the adsorbent weight increased to 23.06 mg (see 'B' and 'C', Figure 25) giving a weight increase of 0.75 mg. In 'D' of Figure 24 , the adsorbent sample is exposed to 300 ºC and nearly returns to its starting weight.

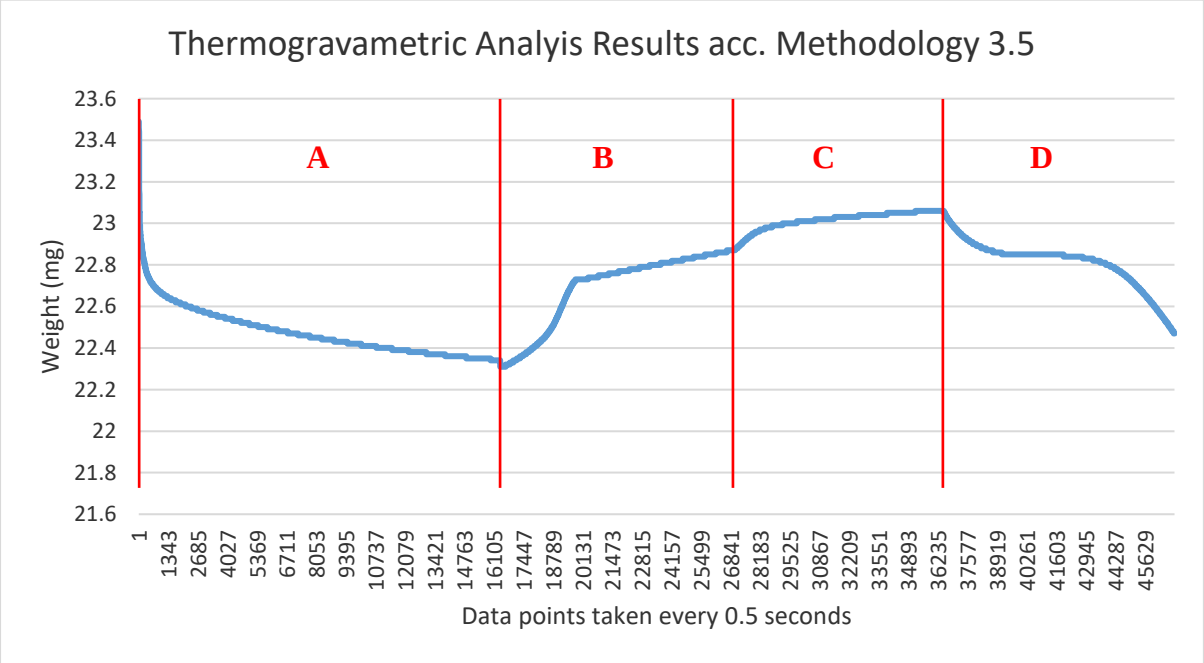

Figure 24: TGA Results

From the Zeochem literature we expected a loading capacity of 1.1 times. As such, with a molecular weight of 28.0134 g/mol and a base weight of 22.31 mg. The expected weight increase would be 0.68 mg. This has been determined with the following Equation:

$$= \left(\frac{28.01 * 1.1}{1}\right) * 22.31/1000 \quad (18)$$

The TGA results recorded a weight increase of 0.75 mg which is ~10% greater than expected.

4.6.1. Thermogravimetric Analysis Results and Discussion

The results of the TGA would suggest that the published data from Zeochem can be relied upon.

To further prove the literature from Zeochem, more experiments can be performed on the TGA. To be able to review different data points on the Zeochem isotherm. Helium can be introduced to replicate different atmospheres when performing Nitrogen loading (see ‘B’ and ‘C’ of Figure 24).

5. CONCLUSIONS; RPSA IN A PORTABLE OXYGEN CONCENTRATOR

5.1. Overview of Conclusions

In this chapter, the main conclusions from the experimental studies conducted in section 4 will be reviewed against the research question proposed in this paper. Considering the limitations of the results, recommendations will be made on how to further develop the research. Finally, the conclusion will suggest how the research can be used to impact the portable oxygen concentrator industry.

5.2. Conclusions

Based on the experimental studies conducted the following conclusions can be drawn:

- From the literature review, one relevant paper was identified by Chai 2011. Experiments were conducted to explore the proposed RPSA and determine a baseline for the current state of the art in literature. The results of the experiments did not match the results of the paper. This was attributed to the length of the column and the use of 90% oxygen artificially inflating the results. As such, this research refutes the results of the Chai 2011 paper. Therefore, the research proposed in this paper will be novel by providing an RPSA system which produces high purity oxygen with a small column.
- The results from breakthrough experiments determined two factors to produce improved results for developing an RPSA. The breakthrough results determined an ideal column length for the cycle. Too small and product purity was reduced by early breakthrough. In addition, the column length can't be indefinitely increased to maximise the product purity. There is a limit where the trade off with increased length just adds unnecessary adsorbent weight. The chosen column length was verified by using it in the initial RPSA experiment. Without changing any parameters, the output purity was increased.
- An experimental set-up allowed for extensive evaluation of an RPSA cycle by design of experiment. Minitab was utilised to determine the appropriate testing regime which allowed for a 2^{nd} order quadratic Equation to be created. From this, the best parameters were determined allowing for a maximum purity of 88.23%

from an output flow of 50 sccm using 2.87 grams of adsorbent. This was an increase of 4 times the current state of the art achieved by industry.

- Throughout the extensive testing it was observed that the adsorbent was beginning to break down and turn into a finer powder. Loading on the adsorbent was understood by measuring pressure drop and calculating it by using the Ergun Equation. It was observed that the Ergun required calibration to the measured results by adjusting the bed void factor to account for the smaller particles. The constant of 0.3 was found to be more agreeable with the results. The calculated and measured results allowed samples to be bulk crush tested. The expected outcome of the larger surface area and load generating more fines was observed.
- Thermogravimetric Analysis experiments were performed on the adsorbent, Zeochems Zeox Z12-49, used throughout the whole research. The TGA experiments matched the isotherm literature produced and published by Zeochem.

5.3. Future Research

Experimental research has provided a solid start to the development of RPSA cycles for use with a small column, low pressure, and low flow, application. However, there were limitations to the results and the following further studies will aide this research:

- Further design of experiments can be performed to hone the cycle and achieve the desired 90% purity output. The research recommended in section 4.4.1 that the purge valve timing, purge flow, and delay should be further analysed.
- When a cycle is finalised. Further reviews should be performed on scaling:
  - adding a second column to increase output with no other changes as the cycle should allow for one column to be filled while one is going through the purge steps
  - increase the column diameter and length incrementally to determine the impact on cycle times and how the output can be increased whilst maintaining purity.
- More TGA experiments should be performed at different environments to confirm the Zeochem data.

- When the data is confirmed. This can be used, alongside the current established data, to create a theoretical model. This could be used to aide and streamline the scaling experiments.
- More crushing testing experiments can be performed. If the same and expected results continue to be observed. A different test method for determining bulk density can be explored. Such as single bead crushing or ball milling could be trialed for comparison. If the results are not as expected. An alternative method to protect the adsorbent can be explored such as coatings.

5.4. Research Question

This research aimed to answer the following:

Can using the RPSA cycle significantly improve oxygen yield per unit volume of adsorbent allowing the development of a small, light POC?

With the target to produce an RPSA system with a significant improvement on the current industries ml per gram of adsorbent, which was calculated as 4.1 ml/g, whilst achieving a 90% oxygen output.

The RPSA developed in this research utilised just 2.87 grams whilst producing 88.23% oxygen at an output flow of 50 sccm. This means the research achieved a ml per gram of 17.42 ml/g which is a 4 times improvement on the current industry best. The research achieved a purity of 88.23%, which is 1.77% below the target. However, with the recommendations in future developments section 5.3 being completed the developed RPSA will reach 90%.

It is the conclusion that the research question has been answered by the extensive experiments and achieved a novelty not currently seen in literature or the portable oxygen concentrator industry.

5.5. Portable Oxygen Concentrator Design

The research proposed in this paper can advance the current state of the art for the POC industry. The are three main criteria defining the industry, per Figure 25, as established in the introduction, for how effective a POC is considered. The output of this research will allow for dramatic improvement in two of the main criteria: reductions in weight for an increased output.

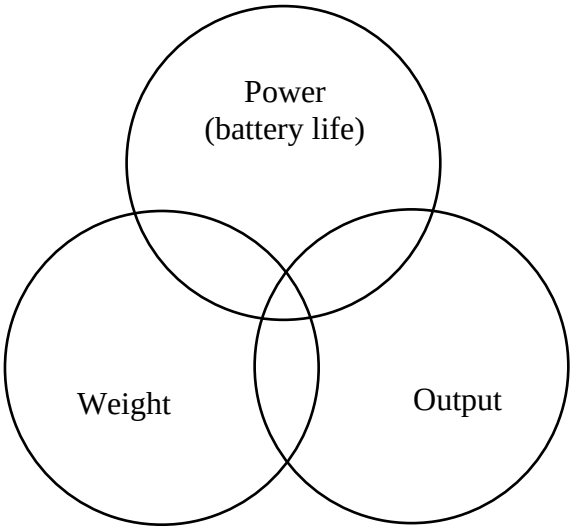

Figure 25: POC Design Criteria Venn Diagram

REFERENNCES

Arvind. R, F. S. (2002). Analysis Of A Piston PSA Process For Air Separation. *Chemical Engineering Science, 57*, 419-433.

Betlem. B. H. L, G. R. (1998). Optimal Operation Of Rapid Pressure Swing Adsorption With Slop Recycling. *Computers And Chemical Engineering, 22*, 633-636.

Buzanowski. M. A, Y. R. (1989). Direct Observation Of The Effects Of Bed Pressure Drop On Adsorption And Desorption Dynamics. *Chemical Engineering Science, 44*, 2392-2394.

Chai. S. W, K. M. (2011). Rapid Pressure Swing Adsorption For Reduction Of Bed Size Factor Of A Medical Oxygen Concentrator. *Industrial And Engineering Chemistry Research, 50*, 8703-8710.

Cheng-Tung Chou, H.-C. W. (1994). Oxygen Enrichment Over Zeolite 5A By A Rapid Pressure Swing Adsorption Process. *Studies in Surface Science And Catalysts, Vol 84*, 1255-1260.

Chiang. A. S. T, H. M. (1995). Radial Flow Rapid Pressure Swing Adsorption. *Adosprtion, 1*, 153-164.

Chronic Obstructive Pulmonary Disease. (2020, September 20). Retrieved from https://www.nhs.uk/conditions/chronic-obstructive-pulmonary-disease-copd/

Chronic Respiratory Diseases. (2020, September 11). Retrieved from https://www.who.int/health-topics/chronic-respiratory-diseases#tab=tab_1

Delgado, J. M. (2006). A Critical Review of Dipsersion in Packed Beds. *Heat Mass Transfer, 42*, 279-310.

E. Alpay, C. N. (1994). Adsorbent Particle Size Effects In The Separation Of Air By Rapid Pressure Swing Adsorption. *Chemical Engineering Science, 49*, 3059-3075.

Edwards. M. F, R. J. (1968). Gas Dispersion In Packed Beds. *Chemical Engineering Science, 23*, 109-123.

Farooq. S, R. D. (1989). Numerical Simulation Of A Pressure Swing Adsorption Oxygen Unit. *Chemical Engineering Science, 44*, 2809-2816.

Farooq. S, R. D. (1990). Heat Effects In Adsorption Column Dynamics. 2 Expermimental Validation Of The One-Dimensional Model. *Industrial And Engineering Chemical Research, 29*, 1084-1090.

Galbraith. (2011). *United States Patent No. US 9,199,055 B2.*

Guerin. (1958). *France Patent No. 3,155,468.*

Gunn. D. J, P. C. (1969). Dispersion In Packed Beds. *Institute Of Chemical Engineers , 47*, 341-350.

Haq. N, R. D. (1985). A Chromatographic Study of Sorption and Diffusion in 5A Zeolite. *Journal of Colloid and Interface Science, 122*, 164-169.

Hart. J, T. W. (1991). Gas Separation By Pulsed Pressure Swing Adsorption. *Gas Separation And Purification, 5*, 125-133.

Home Oxygen Therapy. (2020, September 20). Retrieved from https://www.nhs.uk/conditions/home-oxygen-treatment/

Huang. W. C, C. C. (2003). Comparison Of Radial And Axial Flow Rapid Pressure Swing Adsorption Processes. *Industrial and Engineering Chemistry Research, 42*, 1998-2000.

J, G. D. (1993). On Axial Dispersion In Fixed Beds. *Chemical Engineering and Processing, 32*, 333-338.

J., G. D. (1987). Axial And Radial Dispersion In Fixed Beds. *Chemical Engineering Science, 42*, 363-373.

Jee. J. G, L. J. (2001). Air Separation By A Small-Scale Two-Bed Medical O2 Pressure Swing Adsorption. *Industrial And Engineering Chemistry Research, 40*, 3647-3658.

Jiang. L, B. L. (2003). Simulation And Optimization Of Pressure-Swing Adsorption Systems For Air Separation. *AIChE, 49*, 1140-1157.

Jones. R. L, K. G. (1980). *United States Patent No. 4,194,892.*

Kikkinides. E. S, Y. R. (1993). Effects Of Bed Pressure Drop On Isothermal And Adiabatic Adsorber Dynamics. *Chemical Engineering Science, 48*, 1545-1555.

Ko. D, M. I. (2000). Optimization Of Start-Up Operating Condition In RPSA. *Separation And Purification Technology, 21*, 17-26.

Kopaygorodsky. E. M, G. V. (2004). Predictive Dynamic Model Of Single-Stage Ultra-Rapid Pressure Swing Adsorption. *AIChE, 50*, 953-962.

Kulish. (1998). *United States Patent No. 5,827,258.*

Kulish. (2000). *United States Patent No. 6,068,680.*

LaBuda. (2008). *United States Patent No. US 2008/0083331 A1.*

Langer. G, R. A. (1978). Heat And Mass Transfer In Packed Beds - III. Axial Mass Dispersion. *International Journal Of Heat Mass Transfer, 21*, 751-759.

Lee. (2004). *United States Patent No. US 7,105,038 B2.*

Moran. A, P. M. (2018). Axial Dispersion Effects With Small Diameter Adsorbent Particles. *Adsorption, 24*, 333-344.

Moulijn. J. A, V. S. (1976). The Correlation Of Axial Dispersion Data For Beds Of Small Particles. *Chemical Engineering Science, 31*, 845-847.

Oxygen Concentrator vs.Oxygen Tank. (2024, May 19). Retrieved from https://www.respiratorytherapyzone.com/oxygen-concentrator-vs-oxygen-tank/

Pritchard. C. L, S. G. (1986). Design Of An Oxygen Concentrator Using The Rapid Pressure-Swing Adsorption Principle. *Chemical Engineering Research and Design, 64*, 467-471.

Raghavan, N. S. (1986). Numerical Simulation Of A PSA System Using A Pore Diffusion Model. *Chemical Engineering Science, 41*, 2787-2793.

Rama Rao. V, F. S. (2010). Design Of A Two-Step Pulsed Pressure-Swing Adsorption-Based Oxygen Concentrator. *AIChE, 56*, 354-370.

Rama Rao. V, K. M. (2014). Novel Design And Performance Of A Medical Oxygen Concentrator Using A Rapid Pressure Swing Adsorption Concept. *AIChE Journal, 60*, 3330-3335.

Ruthven, D. M. (1984). *Principles Of Adsorption And Adsorption Processes* (First ed.). John Wiley and Sons.

Ruthven, D. M., & Su, Z. (1993). Diffusion of Oxygen and Nitrogen in 5A Zeolite Crystals and Commercial 5A Pellets. *Chemical Engineering Science*, 3307-3312.

Sereno. C, R. A. (1993). Can Steady-State Momentum Equations Be Used In Modelling Pressurisation Of Adsorption Beds? *Gas Separation And Purification, 7*, 167-173.

Singh. K, J. J. (1997). Numerical Simulation Of Air Separation By Piston-Driven Pressure Swing Adsorption. *Cheimcal Engineering Science, 52*, 3133-3145.

Skarstrom. (1960). *United States Patent No. 2,944,627.*

Smith. A. R, K. J. (2001). A Review Of Air Separation Technologies And Their Intergration With Energy Conversion Processes. *Fuel Processing Technology, 70*, 115-134.

Soo. C. Y, L. Y. (2005). On The Effects Of Axial Dispersion In The Numerical Simulation Of Fast Cycling Adsorption Processes. *Jurnal Teknologi, 43*, 1-13.

Sundaram. N, W. P. (1988). Pressure Drop Effects In The Pressurisation And Blowdown Steps Of Pressure Swing Adsorption. *Chemical Engineering Science, 43*, 123-129.

Suzuki. M, S. J. (1971). Axial Dispersion In Beds Of Small Paticles. *The Chemical Engineering Journal, 3*, 256-264.

Suzuki. M, S. T. (1996). Piston-Driven Ultra Rapid Pressure Swing Adsorption. *Adsorption, 2*, 111-119.

Todd. R. S, W. P. (2006). Mass-Transfer Models For Rapid Pressure Swing Adsorption Simulation. *AIChE, 52*, 3126-3145.

Todd.R. S, W. P. (2005). Pressure Drop In A Packed Bed Under Nonadsorbing And Adsorbing Conditions. *Industrial and Engineering Chemistry Research, 44*, 7234-7241.

Turnock. P. H, K. R. (1971). Separation Of Nitrogen And Methane Via Periodic Adsorption. *AIChE, 17*, 335-342.

WEIHAI. (2018). *China Patent No. CN109173579A.*

Wu. C. W, K. M. (2014). Column Dynamic Study Of Mass Transfer Of Pure N2 and O2 Into Small Particles Of Pelletized LiLSX Zeolite. *Industrial and Engineering Chemistry Research, 53*, 17806-17810.

Wu. C. W, K. M. (2015). Equilibrium Isotherm And Mass Transfer Coefficient For Adsorption Of Pure Argon On Small PArticles Of Pelletized Lithium-Exchanged Low Silica X Zeolite. *Industrial and Engineering Chemistry Research, 54*, 2385-2390.

Yang, R. T. (1987). *Gas Separation By Adsorption Processes* (First ed.). MA: Butterworth Publishers.

Yang. J, P. M. (1998). Effects Of Pressure Drop In A PSA Process. *Korean Journal Of Chemical Engineering, 15*, 211-216.

Z. P. Lu, J. M. (1993). Simulation of A Three-Step One-Column Pressure Swing Adsorption Process. *AIChE Journal*, 1483-1496.

Zhang. Z, G. J. (1998). Separation Of A Nitrogen-Carbon Dioxide Mixture By Rapid Pressure Swing Adsorption. *Adsorption, 4*, 173-177.

Zhong. (2010). *United States Patent No. US 7,828,878 B2.*

Zhu. Z, L. Y. (2016). Study Of A Rapid Vacuum Pressure Swing Adsorption Process With Intermediate Gas Pressurisation For Producing Oxygen. *Adsorption, 23*, 175-184.

APPENDIX A. OXYGEN CONCENTRATOR MARKET REVIEW

Table 18: Oxygen Concentrator Market Review A-B

Manufacturer	Airsep	Airsep	Airsep	Airsep	Beijing North Star Yaao Scitech
Location	United States	United States	United States	United States	China
Device Type	Portable	Portable	Stationary	Stationary	Stationary
Device Family	Focus	FreeStyle	NewLife	VisionAire	FY
Devices	Focus	Freestyle FreeStyle 5	NewLife Elite NewLife Intensity	VisionAire 2 VisionAire 3 VisionAire 5	FY3, FY4, FY5 FY8, FY10
Noise (dBA)	45	38-44	48-50	40	40-56
Average Power Consumption (W)	28	< 120	350	290	380-480
Power Efficiency (W/Lpm)	70	NA	70	58	48-127
Min Oxygen Output Flow Rate	2 (continuous equivalent)	1 (continuous equivalent)	0.13	0.13	0.5
Max Oxygen Output Flow Rate	2 (continuous equivalent)	3.5 (continuous equivalent) 1 Lpm continuous	10	5	3-10
Oxygen Concentration	87-95.6	87-95.5	87-95.5	87-95.5	≥90
Width (mm)	122	155-168	419	358	290-381
Height (mm)	163	218-272	699	528	500-600
Depth (mm)	64	91-112	368	292	310-450
Weight (kg)	0.8	2-2.8	26.3	13.6	21-30

Table 18: Oxygen Concentrator Market Review A-B (Continued)

Manufacturer	Airsep	Airsep	Airsep	Airsep	Beijing North Star Yaao Scitech
Continuous or pulse flow	Pules	Pulse	Continuous	Continuous	Continuous
Notes	The weight does not include the batteries to power the device. https://www.caireinc.com/providers/products/	https://www.caireinc.com/providers/products/	https://www.caireinc.com/providers/products/	https://www.caireinc.com/providers/products/	Not FDA Approved. https://healthmanagement.org/site/p/beijing-north-star-yaao-scitech-co-ltd-1

Table 19: Oxygen Concentrator Market Review B-C

Manufacturer	Beijing North Star Yaao Scitech	Caire	Caire	Canta Medical Tech Co.	Canta Medical Tech Co.
Location	China	United States	United States	China	China
Device Type	Portable	Stationary	Portable	Stationary	Stationary
Device Family	FY600	Companion 5	FreeStyle	HG	V
Devices	FY600	Companion 5	FreeStyle Comfort	HG3, HG5, HG8, HG10	V3, V5, V8
Noise (dBA)	52	40	40	45-50	40-45
Average Power Consumption (W)	Unspecified	250 @ 2 Lpm 350 @ 5 Lpm	350	350-530	350-480
Power Efficiency (W/Lpm)	87	125 @ 2 Lpm 70@ 5 Lpm	70	53-117	60-117
Min Oxygen Output Flow Rate	Unspecified	0.5	0.21	01	1
Max Oxygen Output Flow Rate	0.6	4.6	1.05	3-10	3-8
Oxygen Concentration	≥90	87-95.5	87-95.5	90-96	90-96
Width (mm)	185	318	279	399	391
Height (mm)	135	546	185	650	620
Depth (mm)	343	343	79	366	338
Weight (kg)	4.3kg	16.3	2.7	27-31	21-24
Continuous or pulse flow	Continuous	Continuous	Pulse	Continuous	Continuous

Table 19: Oxygen Concentrator Market Review B-C (Continued)

Manufacturer	Beijing North Star Yaao Scitech	Caire	Caire	Canta Medical Tech Co.	Canta Medical Tech Co.
Notes and Information Source	Not FDA Approved https://healthmanagement.org/site/p/beijing-north-star-yaao-scitech-co-ltd-1	https://www.caireinc.com/product/caire-companion-5/	Caire and Airsep are one company. https://www.caireinc.com/product/freestyle-comfort/	https://www.cantamedical.com/	https://www.cantamedical.com/

Table 20: Oxygen Concentrator Market Review C-D

Manufacturer	Canta Medical Tech Co.	Chart SeQual Technologies	Delphi	DeVilbiss	DeVilbiss
Location	United States	United States	United States	United States	United States
Device Type	Stationary	Portable	Portable	Stationary	Tank Filler
Device Family	Mini	SeQual	Evo Central Air	525 Series	iFill
Devices	M2	eQuinox Eclipse 5 Eclipse 3	RS-00400	525DS 525KS 525PS	535D
Noise (dBA)	40	37-47	43	48	50
Average Power Consumption (W)	90	110	120	310	400
Power Efficiency (W/Lpm)	90	37	Not Disclosed	62	210
Min Oxygen Output Flow Rate	1 (continuous equivalent)	0.5	0.2	0.5	Not Disclosed
Max Oxygen Output Flow Rate	5 (continuous equivalent)	5	0.9	5	1.9
Oxygen Concentration	90-96	87-93	87-93	90-96	90-96
Width (mm)	199	277-290	188	343	311
Height (mm)	324	356-455	295	622	724
Depth (mm)	320	180-201	117	305	572
Weight (kg)	6	6.4-8.2	4.5	16.3	30
Continuous or pulse flow	Pulse	Both	Not Disclosed	Continuous	NA
Notes	Caire and Airsep are one company. https://www.cantamedical.com/	Caire and Chart SeQual Technologies are the same company. https://www.caireinc.com/product/sequal-eclipse-5/	Not OEM. Owned by Oxus Korea. 510(k) Premarket Notification (fda.gov)	Oxygen Therapy (drivedevilbiss.co.uk)	Oxygen Therapy (drivedevilbiss.co.uk)

Table 21: Oxygen Concentrator Market Review D-I

Manufacturer	DeVilbiss	Drive Medical	Drive Medical	GCE LTD	Inogen
Location	United States	United States	United States	UK	United States
Device Type	Portable	Stationary	Stationary	Portable	Stationary
Device Family	iGo2	Pure	Solstice	Zen-O	At Home
Devices	306DS	Pure	18050 18055	Zen-O Zen-O Lite	Inogen At Home
Noise (dBA)	48	45	45-47	38	Not Disclosed
Average Power Consumption (W)	< 120	360-390	300	120-150	275
Power Efficiency (W/Lpm)	Not Disclosed	72-78	60	75	50-55
Min Oxygen Output Flow Rate	0.2	0.5	1	0.2	1
Max Oxygen Output Flow Rate	1.01	5	5	2	5
Oxygen Concentration	88-94	87-96	91-95	87-96	87-96
Width (mm)	279	425	356	212-249	330
Height (mm)	381	622	588	235-313	419
Depth (mm)	203	262	305	97-168	17.8
Weight (kg)	4.95	15.9	16.8	2.5-4.66	8.2
Continuous or pulse flow	Both	Continuous	Continuous	Both	Continuous
Notes	Oxygen Therapy (drivedevilbiss.co.uk)	DeVilbiss and Drive are the same company. Oxygen Therapy (drivedevilbiss.co.uk)	DeVilbiss and Drive are the same company. Oxygen Therapy (drivedevilbiss.co.uk)	https://gcehealthcare.com/products-services/homecare/	https://provider.inogen.com/en

Table 22: Oxygen Concentrator Market Review I

Manufacturer	**Inogen**	**Inova Labs Inc**	**Inova Labs Inc**	**Invacare**	**Invacare**
Location	United States	United States	United States	United States	United States
Device Type	Portable	Portable	Stationary	TankFiller	Stationary
Device Family	One	LifeChoice	Activox	Homefill II	Perfect O2
Devices	G2, G3, G4, G5	Activeox Pro, Activeox Sport	DUO2	IOH200	PerfectO2, PerfectO2 V PerfectO2 W
Noise (dBA)	38-42	41-46	45	Not Disclosed	43
Average Power Consumption (W)	85-90	40	372	140	280-325
Power Efficiency (W/Lpm)	65-69	Not Disclosed	74	Not Disclosed	65
Min Oxygen Output Flow Rate	0.2	0.1	1	0	0.5
Max Oxygen Output Flow Rate	1.3	0.03	5	2	5
Oxygen Concentration	87-96	87-93	90-96	>90	87-95.6
Width (mm)	68-99	231	360	516	381
Height (mm)	150-241	201	630	381	584
Depth (mm)	180-272	109	370	406	305
Weight (kg)	1.2-3.2	2.2	17	15	18.1-20.4
Continuous or pulse flow	Both	Pulse	Continuous	Not Disclosed	Continuous
Notes	https://provider.inogen.com/en	https://www.oxygenconcentratorstore.com/lifechoice-activox/	https://www.oxygenconcentratorstore.com/lifechoice-activox/	https://www.lincare.com/en/services/home-oxygen-therapy	https://www.lincare.com/en/services/home-oxygen-therapy

Table 23: Oxygen Concentrator Market Review I-K

Manufacturer	**Invacare**	**Invacare**	**Kare Medical**	**Kare Medical**	**Kroeber**
Location	United States	United States	Turkey	Turkey	Germany
Device Type	Stationary	Portable	Stationary	Stationary	Stationary
Device Family	Platinum	XPO2, SOLO2	OxyBreath	OxyBreath Mini	Aeroplus
Devices	Platinum XL Platinum 5 Platinum9 Platinum 10	POC1-100C, POC1-100B TPO100, TPO100B XPO100, XPO100B	Oxybreath 10L	Mini 3 Mini 5	5
Noise (dBA)	50	40-45	Not Disclosed	Not Disclosed	<40
Average Power Consumption (W)	585	36	550	165-330	295
Power Efficiency (W/Lpm)	59	45	55	55-66	59
Min Oxygen Output Flow Rate	0.5	0.3	1	3-5	0.5
Max Oxygen Output Flow Rate	10	0.8	10	Not Disclosed	5
Oxygen Concentration	87-94	87-95.6	89-95 (1-9 Lpm) 87-93 (10 Lpm)	90-96	82-95
Width (mm)	467	178-190.5	Not Disclosed	Not Disclosed	290
Height (mm)	670	240-254	Not Disclosed	Not Disclosed	599
Depth (mm)	365	98.5-102	Not Disclosed	Not Disclosed	399
Weight (kg)	24.5	2.18-17	21.7	12-15.1	15
Continuous or pulse flow	Continuous	Continuous	Continuous	Continuous	Continuous

Table 23: Oxygen Concentrator Market Review I-K (Continued)

Manufacturer	Invacare	Invacare	Kare Medical	Kare Medical	Kroeber
Notes	https://www.lincare.com/en/services/home-oxygen-therapy	https://www.lincare.com/en/services/home-oxygen-therapyhttps://www.lincare.com/en/services/home-oxygen-therapy	http://karemedical.co/en/	http://karemedical.co/en/	https://kroeber.de/o2_oxygentherapy.php

Table 24: Oxygen Concentrator Market Review K-L

Manufacturer	Kroeber	Kroeber	Kroeber	Legend Medical	Legend Medical
Location	Germany	Germany	Germany	China	China
Device Type	PorTable	Stationary	Stationary	PorTable	Stationary
Device Family	Aeroplus	Krober	Topair	LoveGo	LG103
Devices	M	O2 4.0	2	LoveGo Legend PorTable	LG103
Noise (dBA)	40	31-35	<45	38-40	Not Disclosed
Average Power Consumption (W)	Max 100	280-350	790	90	Not Disclosed
Power Efficiency (W/Lpm)	125	56-58	66	72	Not Disclosed
Min Oxygen Output Flow Rate	0.2	1	1.5	1	1
Max Oxygen Output Flow Rate	0.8	5-6	12	3-5	7
Oxygen Concentration	>90	72-95	82-95	40-93	90-96
Width (mm)	155	203	404	110-244	208
Height (mm)	231	521	541	170-363	299
Depth (mm)	249	533	516	180-260	378
Weight (kg)	3.6	16-20	45	2.4-5.4	15
Continuous or pulse flow	Pulse, Quasi Continuous	Continuous	Continuous	Continuous	Both
Notes	https://kroeber.de/o2_oxygentherapy.php	https://kroeber.de/o2_oxygentherapy.php	https://kroeber.de/o2_oxygentherapy.php (kroeber.de)	https://lovegomedical.com/	https://lovegomedical.com/

Table 25: Oxygen Concentrator Market Review L-M

Manufacturer	Longfei	Longfian	Longfian Scitech	Medicap	Metran
Location	China	China	China	Germany	Japan
Device Type	Stationary	PorTable	Stationary	Stationary	PorTable
Device Family	LFY	Jay	JAY	PRECISE 6000	KM-X3L
Devices	LFY-I-3A, B, F, G LFY-I-4A, B LFY-I-5A, B, F LFY-I-8A, B	1P 3P 5P	JAY-3 JAY-5 JAY-8 JAY-10	P 6000 P 6000 S	KM-X3L
Noise (dBA)	<48-62	45	43-50	39	33
Average Power Consumption (W)	300-520	75	280-550	<460	45
Power Efficiency (W/Lpm)	90-104	Not Disclosed	55-93	77	45
Min Oxygen Output Flow Rate	1	1	0.13	0.1	Not Disclosed
Max Oxygen Output Flow Rate	3.8	5	3-10	5-6	1
Oxygen Concentration	90-96	30-90	88-96	77-95	87-93
Width (mm)	480	191	376	215	269
Height (mm)	730	320	599	550	320
Depth (mm)	500	351	366	550	191
Weight (kg)	20-28.5	6	14-30	21	5.8
Continuous or pulse flow	Continuous	Not Disclosed	Continuous	Continuous	Both
Notes	Zhejiang Longfei Medical Instrument Co., Ltd_Others	Zhejiang Longfei Medical Instrument Co., Ltd_Others	Zhejiang Longfei Medical Instrument Co., Ltd_Others	Oxygen therapy, altitude therapy, inhalation - medicap Webseite!	metran.co.jp/en/

Table 26: Oxygen Concentrator Market Review N-P

Manufacturer	**Nidek**	**O2 Concepts**	**O2 Concepts**	**Phillips Respironics**	**Phillips Respironics**
Location	United States	United States	United States	United States	United States
Device Type	Stationary	PorTable	PorTable	Stationary	PorTable
Device Family	Nuvo	OxLife Independence	Freedom	Everflo	SimplyGo
Devices	Nuvo Lite, Nuvo 8	OxLife	Freedom	Everflo, Everflo Q	SimplyGo, SimplyFlo
Noise (dBA)	40-48	41-44	56	40	43
Average Power Consumption (W)	350-500	Not Disclosed	Not Disclosed	350	120
Power Efficiency (W/Lpm)	63-70	Not Disclosed	Not Disclosed	70	60
Min Oxygen Output Flow Rate	0.5	0.5	0.12	0.5	0.5
Max Oxygen Output Flow Rate	5-8	3	0.6	5	2
Oxygen Concentration	87-93	87-95	87-95	90-96	87-96
Width (mm)	396	203	228	381	292
Height (mm)	706	305	238	584	254
Depth (mm)	394	203	86	241	152
Weight (kg)	14.5-25.2	42.4	2.66	14.1	3.8-4.5
Continuous or pulse flow	Continuous	Both	Pulse	Continuous	Pulse
Notes	https://nidekmedical.com/	O2 Concepts (o2-concepts.com)	O2 Concepts (o2-concepts.com)	https://www.philips.co.uk/healthcare/solutions/sleep-and-respiratory-care/oxygen/porTable-oxygen	https://www.philips.co.uk/healthcare/solutions/sleep-and-respiratory-care/oxygen/porTable-oxygen

Table 27: Oxygen Concentrator Market Review P-#

Manufacturer	**Phillips Respironics**	**Phillips Respironics**	**Precision Medical**	**Precision Medical**	**Vbox Inc**	**3B Products**
Location	United States	United States	United States	United States	United States	United States
Device Type	Portable	Portable	Portable	Portable	Portable	Portable
Device Family	SimplyGo	Millennium M10	Easy Pulse	Live Active Five	Trooper	Aer X
Devices	SimplyGo Mini	Millennium M10	PM4130 PM4145	Live Active Five	Trooper	Aer X
Noise (dBA)	46	50	40.6-42	40-48	43	40
Average Power Consumption (W)	120	600	120	100	Not Disclosed	Not Disclosed
Power Efficiency (W/Lpm)	>55	60	171	100	Not Disclosed	Not Disclosed
Min Oxygen Output Flow Rate	0.22	1	0.2	0.2	1	0.3
Max Oxygen Output Flow Rate	1	10	0.7	1	5	1
Oxygen Concentration	87-96	88-96	87-95	87-95.5	>87	87-94
Width (mm)	211	483	165	216	71	212
Height (mm)	239-259	686	216-257	214	184	183
Depth (mm)	91	330	114	83	152	67
Weight (kg)	2.3-2.7	24.1	4.91-5.6	2.2	1.7	1.9
Continuous or pulse flow	Pulse	Continuous	Pulse	Pulse	Pulse	Pulse

Table 27: Oxygen Concentrator Market Review J (Continued)

Manufacturer	Phillips Respironics	Phillips Respironics	Precision Medical	Precision Medical	Vbox Inc	3B Products
Notes	https://www.philips.co.uk/healthcare/solutions/sleep-and-respiratory-care/oxygen/porTable-oxygen	https://www.philips.co.uk/healthcare/solutions/sleep-and-respiratory-care/oxygen/porTable-oxygen	https://precisionmedical.com/oxygen-concentrators/	https://precisionmedical.com/oxygen-concentrators/	Vbox was purchased by 3B Products	https://www.vitalitymedical.com/3b-aer-x-porTable-oxygen-concentrator.html

APPENDIX B. REVIEW OF PPSA AND RPSA LITERATURE

Table 28: Review PPSA and RPSA Literature

Author	Cycle mode	Particle (mm)	Cycle Time (s)	Input flow Rate (Lpm)	Output flow rate (Lpm)	Output purity %	Recovery %	Pressure (Kpa)	Temperature (K)	Column size length x diameter (mm)	Notes
Turnock (1971)	PPSA	42-60 mesh particles 5A Zeolite	0.05-0.4 cycles	Not Disclosed	Not Disclosed	Not Disclosed	Not Disclosed	68.94-206.84	297.15	1524x228.6	Rapid cycling significantly improved the nitrogen enrichment at the expense of low recovery
Jones (1980)	RPSA	20-120 Mesh Particle zeolite	0.2-5 feed, 0.3 delay 1-9 exhaust	3.7-7.8	0.15-0.433	60-94.4	9-24.5	55.15-206.84	Not Disclosed	381-1523x25.4-76.2	Aim of invention was to improve product recovery for RPSA. This was achieved with a desorption time twice the length of adsorption time. They also demonstrated a fivefold increase in oxygen productivity per unit mass of adsorbent.
Pritchard (1986)	RPSA	40-60 mesh and 60-80 mesh 5A Zeolite	Pressurisation 0.1, Feed 1, Delay 0.5, Depressurisation 0.1, exhaust 4	Not Disclosed	2 l/min	30/40	44.3	14-22 (0.14-0.22 bar)	Not Disclosed	230x38	Although the desired enrichment was reached a pressure drop at the feed end was seen after closing the feed valve. This shows the adsorbent has not reached full saturation.
Hart and Thomas (1991)	PPSA	0.25-0.5mm activated carbon	2 feed, 8 exhaust	0.0242-0.038	Not Disclosed	72	10.2	100-380	293.15	Not Disclosed	The separation factor would increase, and product recovery would decrease as feed pressure was increased

Table 28: Review PPSA and RPSA Literature (Continued)

Author	Cycle mode	Particle (mm)	Cycle Time (s)	Input flow Rate (Lpm)	Output flow rate (Lpm)	Output purity %	Recovery %	Pressure (KPa)	Temperature (K)	Column size length x diameter (mm)	Notes
Alpay and Scott (1992)	Not Disclosed	0.15-0.25, 0.25-0.35, 0.35-0.42 and 0. 50-0.71	3 total with a feed to cycle time ration of 0.5	4.2-13.92	Not Disclosed	49.8-76.6	6.3-45.3	Not Disclosed	290K	1000x73	First paper to focus on particle size rather than cycle time. They concluded that particles of 250 to 350 microns gave the best oxygen purity.
Baron (1993)	RPSA	0.2-0.5mm 5a molecular sieve	1 feed, 2-3 delay 5 exhaust	Not Disclosed	Not Disclosed	Not Disclosed	Not Disclosed	Not Disclosed	Not Disclosed	1000-2000	The RPSA process performs the same steps as the multi-column PSA process, but in a single bed: pressurization, adsorption, depressurization and desorption. With surge tanks in feed and product lines, RPSA accepts continuous flows. Multiple columns operating in alternation as in PSA are not needed and this leads to a simpler process with lower investment.
Lu (1993)	RPSA	Not Disclosed	Not Disclosed	Not Disclosed	Not Disclosed	Not Disclosed	Not Disclosed	Not Disclosed	298K	1000	Displayed that separation performance decreased with the empty volume at the feed end and slightly increased with the empty volume at the product end.

Table 28: Review PPSA and RPSA Literature (Continued)

Author	Cycle mode	Particle (mm)	Cycle Time (s)	Input flow Rate (Lpm)	Output flow rate (Lpm)	Output purity %	Recovery %	Pressure (KPa)	Temperature (K)	Column size length x diameter (mm)	Notes
Chou and Wu (1994)	RPSA	60-80 mesh powder.	Feed 2 Delay 0.5	Not Disclosed	0.25-1	92	10	137.89-241.31	Not Disclosed	508x55	Observed that an increase in feed pressure increased the product purity and adsorbent productivity. The recovery was not changed by feed pressure but by the timings. The recovery was improved by the addition of a delay, as seen by jones and only up to 0.5s. Greater than this decreased the recovery.
Chiang and Hong (1995)	Radial RPSA	60-80 mesh, 200-325 mesh, 0.003 powder	Feed 4 Delay 1 Exhaust 12	100-200	1.499-1.968	60	6.94-14.79	137.89	Not Disclosed	200x75	They found the radial system reduced the pressure drop so much that the breakthrough was almost instantaneous, and the system requires very small particles to provide a pressure drop.
Zhang (1998)	RPSA	0.44mm silica gel particle	Feed 1.5 desorption 2	Not Disclosed	Not Disclosed	89.5	70	1000	303.15	1600x20	Explored using two column RPSA. Showed that changing the times increased purity but decreased purity. Increasing feed pressure improved purity, recovery and productivity.

Table 28: Review PPSA and RPSA Literature (Continued)

Author	Cycle mode	Particle (mm)	Cycle Time (s)	Input flow Rate (Lpm)	Output flow rate (Lpm)	Output purity %	Recovery %	Pressure (KPa)	Temperature (K)	Column size length x diameter (mm)	Notes
Betlem (1998)	RPSA	0.1-0.5	Not Disclosed	30	2-5	90	Not Disclosed	137.89-344.73	Not Disclosed	1000-1500	Due to the short cycle times the process is nearly isothermal. Explored recycling the product and the exhaust which improved productivity and recovery.
Kulish and Swank (1998)	Rotary RPSA	Not Disclosed	1-2 feed 5-10 desorption	Not Disclosed	Not Disclosed	Not Disclosed	Not Disclosed	Not Disclosed	Not Disclosed	No length provided but volume given as 50000mm^3	Used multiple beds.
Huang and Chou (2003)	Radial RPSA	5a Zeolite	Not Disclosed	100	0.24	97	12	154-182.38	298K	1800x300	Showed that radial RPSA had the advantage of a lower pressure drop.
Soo (2005)	Not Disclosed	Not Disclosed	Not Disclosed	Not Disclosed	Not Disclosed	Not Disclosed	Not Disclosed	Not Disclosed	Not Disclosed	Not Disclosed	Theoretically reviewed the effect of axial dispersion on the performance of fast cycling. An increase in axial dispersion reduced purity.

Table 28: Review PPSA and RPSA Literature (Continued)

Author	Cycle mode	Particle (mm)	Cycle Time (s)	Input flow Rate (Lpm)	Output flow rate (Lpm)	Output purity %	Recovery %	Pressure (KPa)	Temperature (K)	Column size length x diameter (mm)	Notes
Todd and Webley (2006)	RPSA	LiLSX Zeochem	Totally cycle time 8-50	Not Disclosed	Not Disclosed	Not Disclosed	Not Disclosed	300	290K	1000x156	Compared DGM and LDF models for simulating RPSA. At long cycle times both models matched experimental results where kinetics of diffusion were not important. During short cycle times the LDF model under predicted the experimental performance. Times above 50 seconds are not considered RPSA.
LaBuda (2008)	RPSA	Not Disclosed	Total cycle time 45-90	Not Disclosed	Not Disclosed	Not Disclosed	Not Disclosed	Not Disclosed	Not Disclosed	Not Disclosed	Is a patent more concerned with the addition of a desiccant than a major RPSA development. The cycle times are too high to be RPSA
Zhong (2010)	RPVSA	Not Disclosed	Not Disclosed	Not Disclosed	Not Disclosed	Not Disclosed	Not Disclosed	Not Disclosed	Not Disclosed	Not Disclosed	Is a patent to propose particle size, bed length and cycle time to make axial dispersion the dominating factor over pore resistance.

Table 28: Review PPSA and RPSA Literature (Continued)

Author	Cycle mode	Particle (mm)	Cycle Time (s)	Input flow Rate (Lpm)	Output flow rate (Lpm)	Output purity %	Recovery %	Pressure (KPa)	Temperature (K)	Column size length x diameter (mm)	Notes
Rama (2010)	RPSA	0.001-0.4	Not Disclosed	Not Disclosed	Not Disclosed	Not Disclosed	Not Disclosed	151-1063.91	298.15K	4-6000	
Chai (2011)	RPSA	0.35- 0.45	Total cycle time 2-10	Not Disclosed	Not Disclosed	90	Not Disclosed	202-400	Not Disclosed	104x40	Proposed a concentrator which would snap on to an airline to produce a continuous high purity oxygen.
Rama (2014)	Snap-on RPSA	UOP Oxysiv MDX 0.35 particle	Total cycle time 5-6	110	1-3	90	27	400	Not Disclosed	127x40	Investigated using the product gas to partially pressurise the column. This improved the recovery and reduced the volume of required zeolite

APPENDIX C. CRUSH TEST FIXTURE DRAWINGS

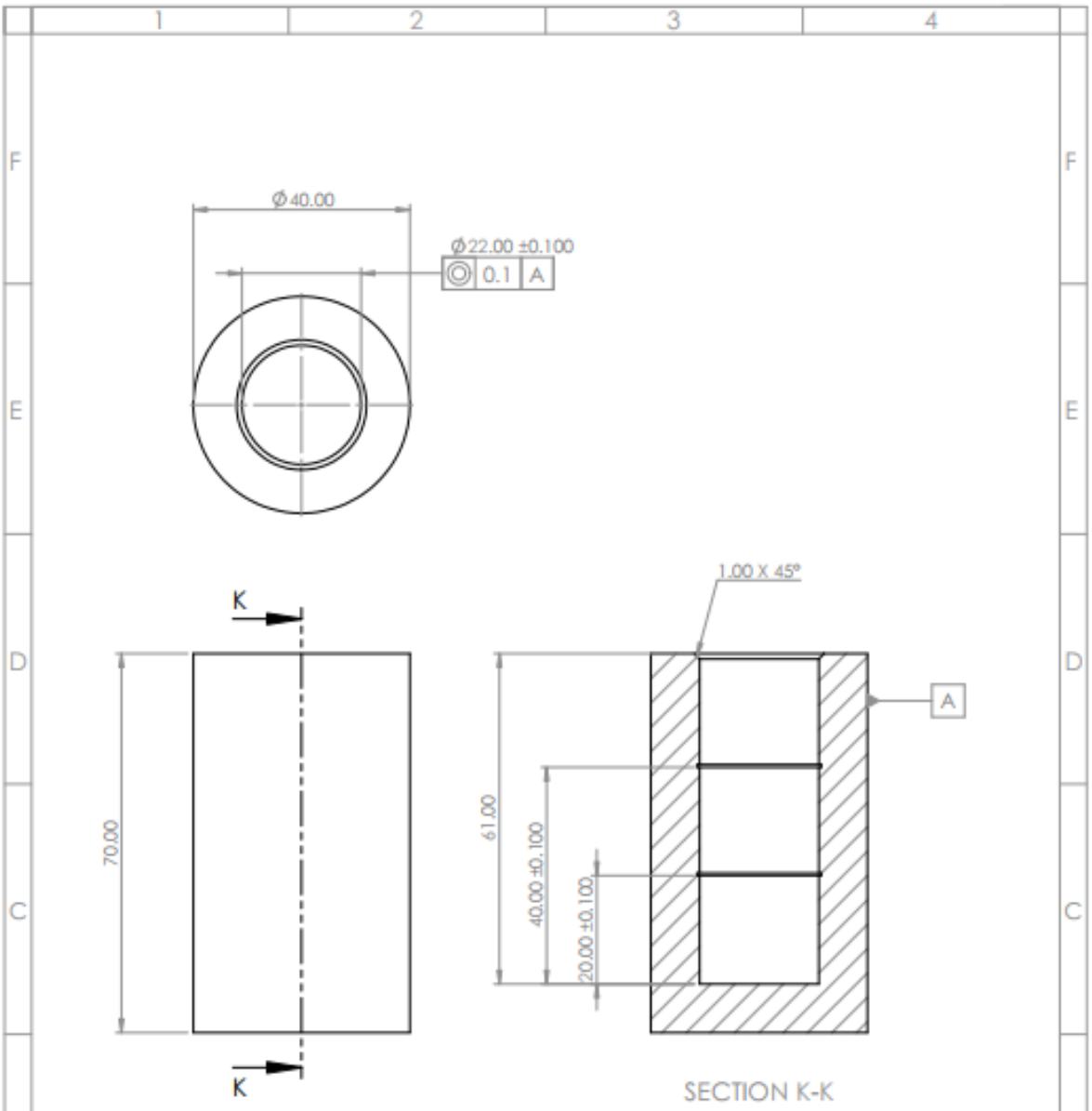

NOTES:

1. MATERIAL - ALUMINIUM BAR - GRADE CHOSEN TO REFLECT PRICE
2. BREAK ALL SHARP CORNERS
3. SCORE INSIDE THE BORE AT THE HEIGHTS OF 20MM AND 40MM

REV.	DATE	DESCRIPTION	ECO NUMBER	RELEASED BY
A	17/01/2022	INITIAL RELEASE		CK

MATERIAL:	Material <not specified>
DRAWN DATE:	6/10/2022
DRAWN BY:	C. KENNY
PART SIMILAR TO:	
APPROVED BY:	G. PEMBERTON
PROCESS:	
SURFACE FINISH UNLESS OTHERWISE STATED	0.3umRa
SHEET SCALE	1:1
CRITICAL DIMENSIONS MARKED	
GCE QUALITY APPLIES UNLESS OTHERWISE STATED	
TOLERANCE UNLESS OTHERWISE STATED	ISO 2768 m,K
WEIGHT	64.71g

Zeolite Crush Test Fixture - H22

DEV01288 - h22

REVISION: A

SHEET No. / OF: 1/1

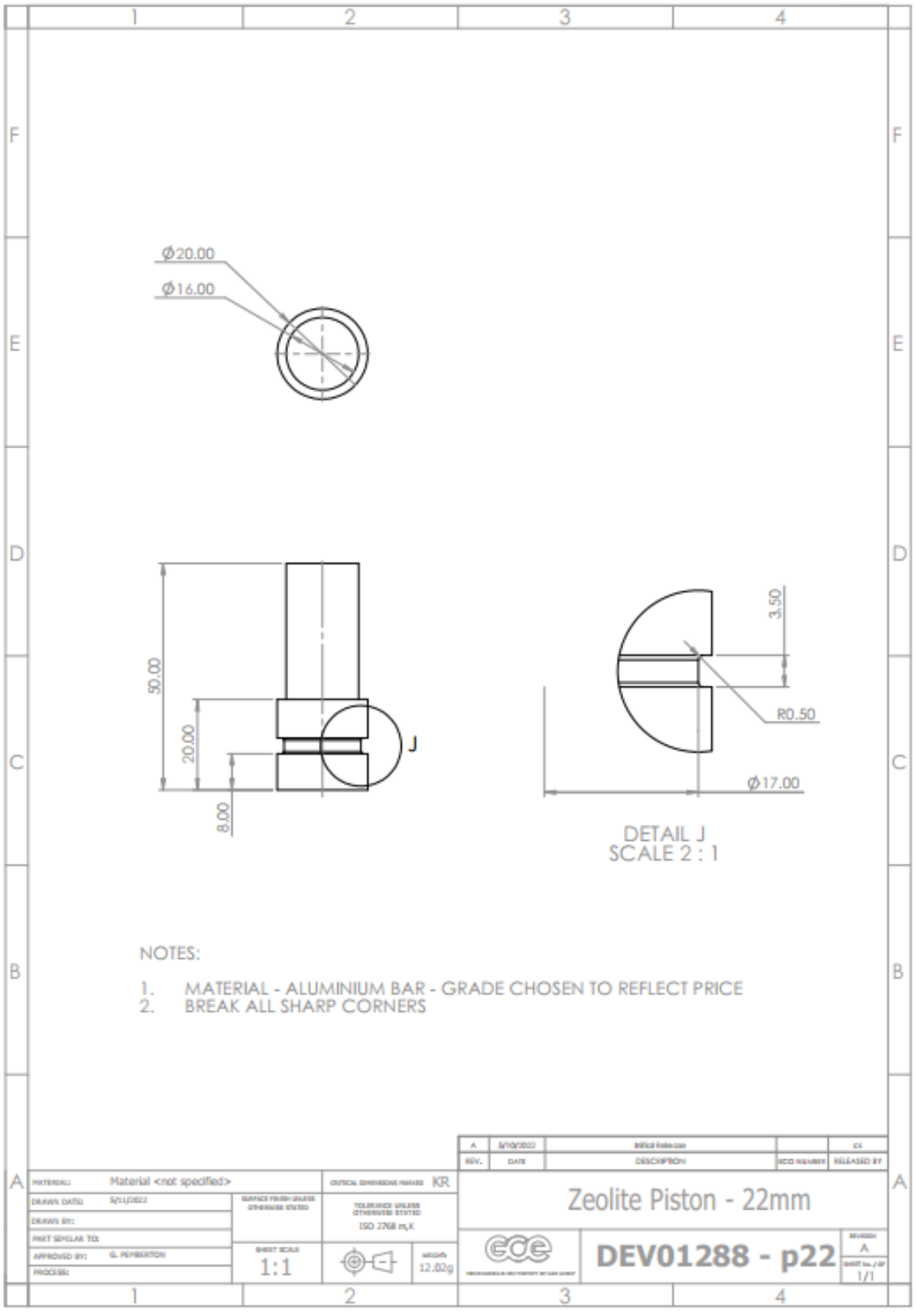
Ø20.00
Ø16.00
50.00
20.00
8.00
J
3.50
R0.50
Ø17.00
DETAIL J
SCALE 2 : 1
NOTES:
1. MATERIAL - ALUMINIUM BAR - GRADE CHOSEN TO REFLECT PRICE
2. BREAK ALL SHARP CORNERS
Material <not specified>
KR
Zeolite Piston - 22mm
ISO 2768 m,K
1:1
12.02g
DEV01288 - p22
A
1/1

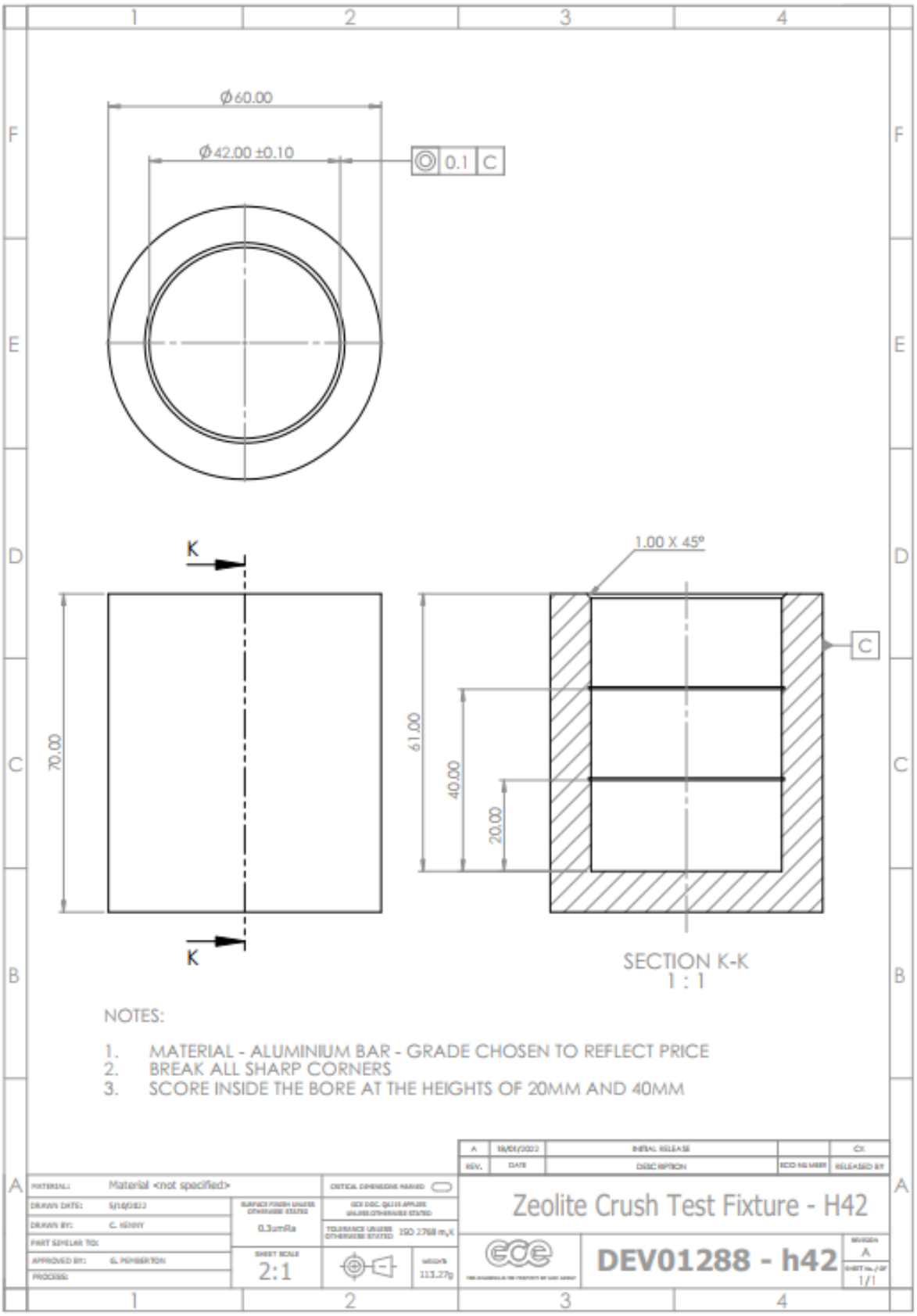
Ø60.00
Ø42.00 ±0.10
0.1 C
K
K
70.00
1.00 X 45°
C
61.00
40.00
20.00
SECTION K-K
1 : 1
NOTES:
1. MATERIAL - ALUMINIUM BAR - GRADE CHOSEN TO REFLECT PRICE
2. BREAK ALL SHARP CORNERS
3. SCORE INSIDE THE BORE AT THE HEIGHTS OF 20MM AND 40MM
A 19/01/2022 INITIAL RELEASE CK
REV. DATE DESCRIPTION ECO NO. RELEASED BY
MATERIAL: Material <not specified>
DRAWN DATE: 5/19/2022
DRAWN BY: C. KENNY
PART SIMILAR TO:
APPROVED BY: G. POWDERTON
PROCESS:
SURFACE FINISH UNLESS OTHERWISE STATED 0.3umRa
SHEET SCALE 2:1
CRITICAL DIMENSIONS MARKED
TOLERANCE UNLESS OTHERWISE STATED ISO 2768 m,K
WEIGHT 113.27g
Zeolite Crush Test Fixture - H42
DEV01288 - h42
REVISION A
SHEET No. / OF 1/1

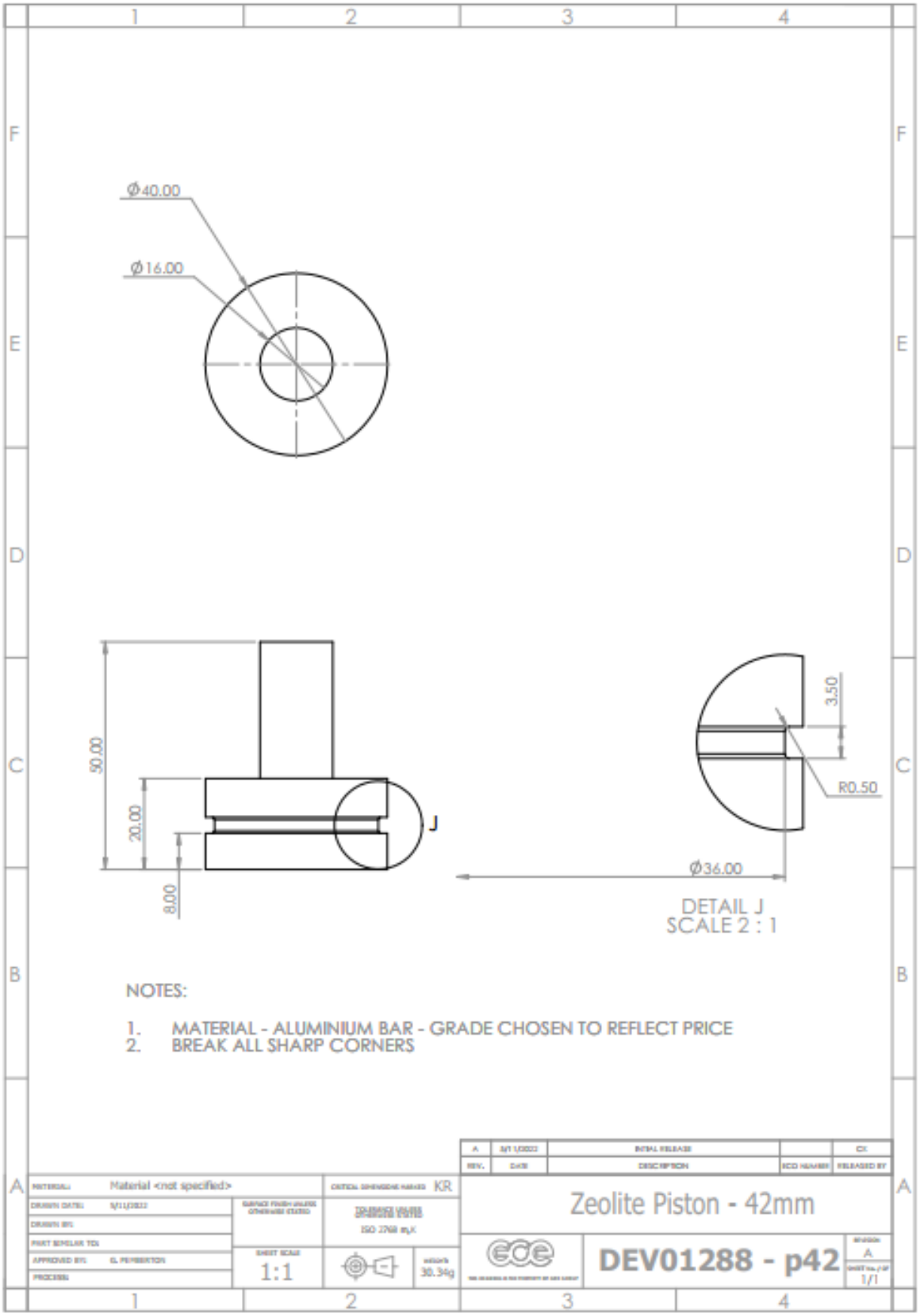
Ø40.00
Ø16.00
50.00
20.00
8.00
J
3.50
R0.50
Ø36.00
DETAIL J
SCALE 2 : 1
NOTES:
1. MATERIAL - ALUMINIUM BAR - GRADE CHOSEN TO REFLECT PRICE
2. BREAK ALL SHARP CORNERS
Material <not specified>
KR
Zeolite Piston - 42mm
DEV01288 - p42
1:1
30.34g

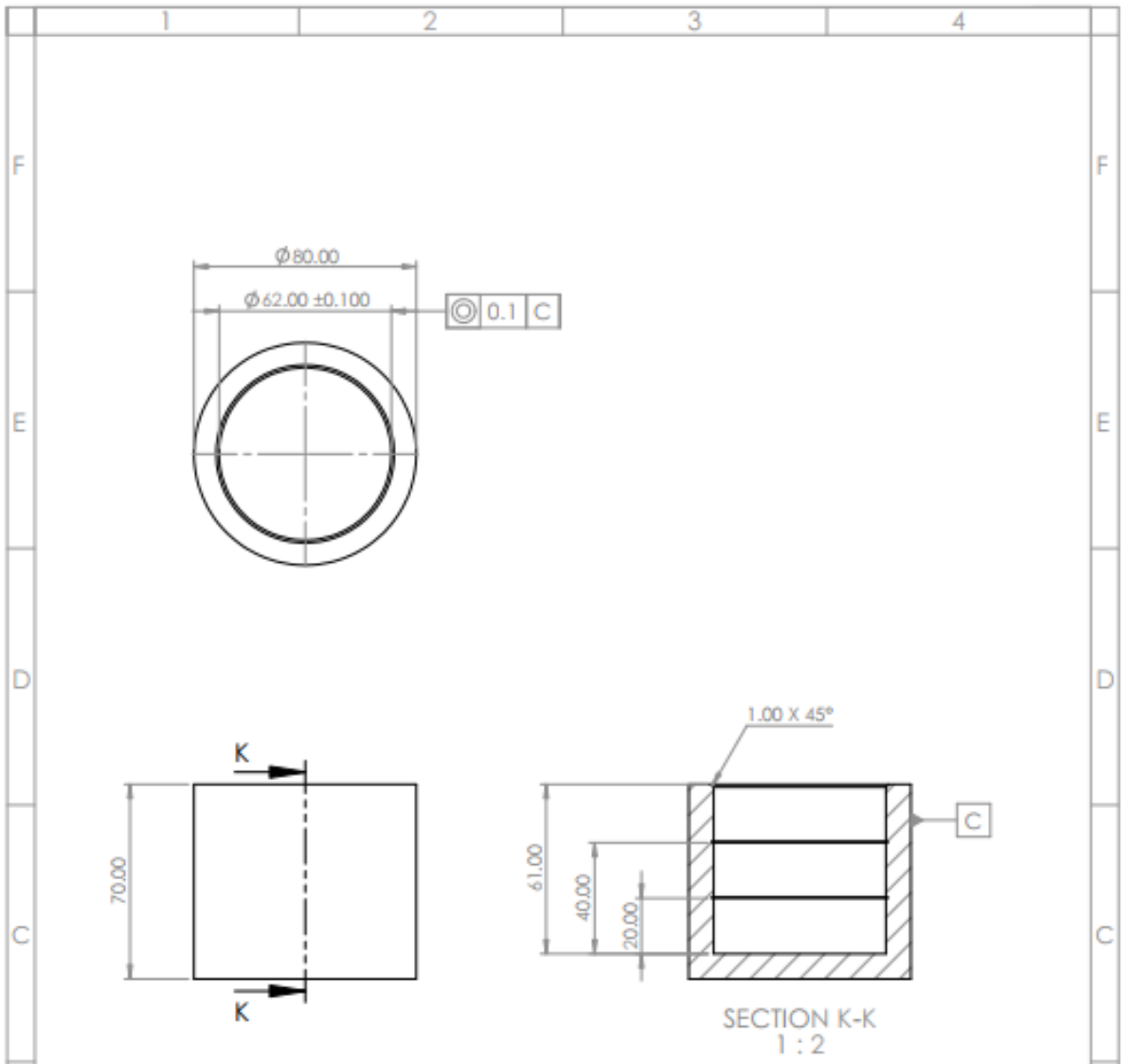

NOTES:

1. MATERIAL - ALUMINIUM BAR - GRADE CHOSEN TO REFLECT PRICE
2. BREAK ALL SHARP CORNERS
3. SCORE INSIDE THE BORE AT THE HEIGHTS OF 20MM AND 40MM

REV.	DATE	DESCRIPTION	ECO NUMBER	RELEASED BY
A	18/01/2022	INITIAL RELEASE		CK

MATERIAL:	Material <not specified>
DRAWN DATE:	6/10/2022
DRAWN BY:	L.YATES
PART SIMILAR TO:	
APPROVED BY:	C. PHILIPS
PROCESS:	
SURFACE FINISH UNLESS OTHERWISE STATED	0.3umRa
SHEET SCALE	2:1
CRITICAL DIMENSIONS MARKED	
ECO DOC. QUOTE APPLIES UNLESS OTHERWISE STATED	
TOLERANCE UNLESS OTHERWISE STATED	ISO 2768 m,K
WEIGHT	167.50g

Zeolite Crush Test Fixture - H62

ece

DEV01288 - h62

REVISION: A

SHEET No. | OF: 1/1

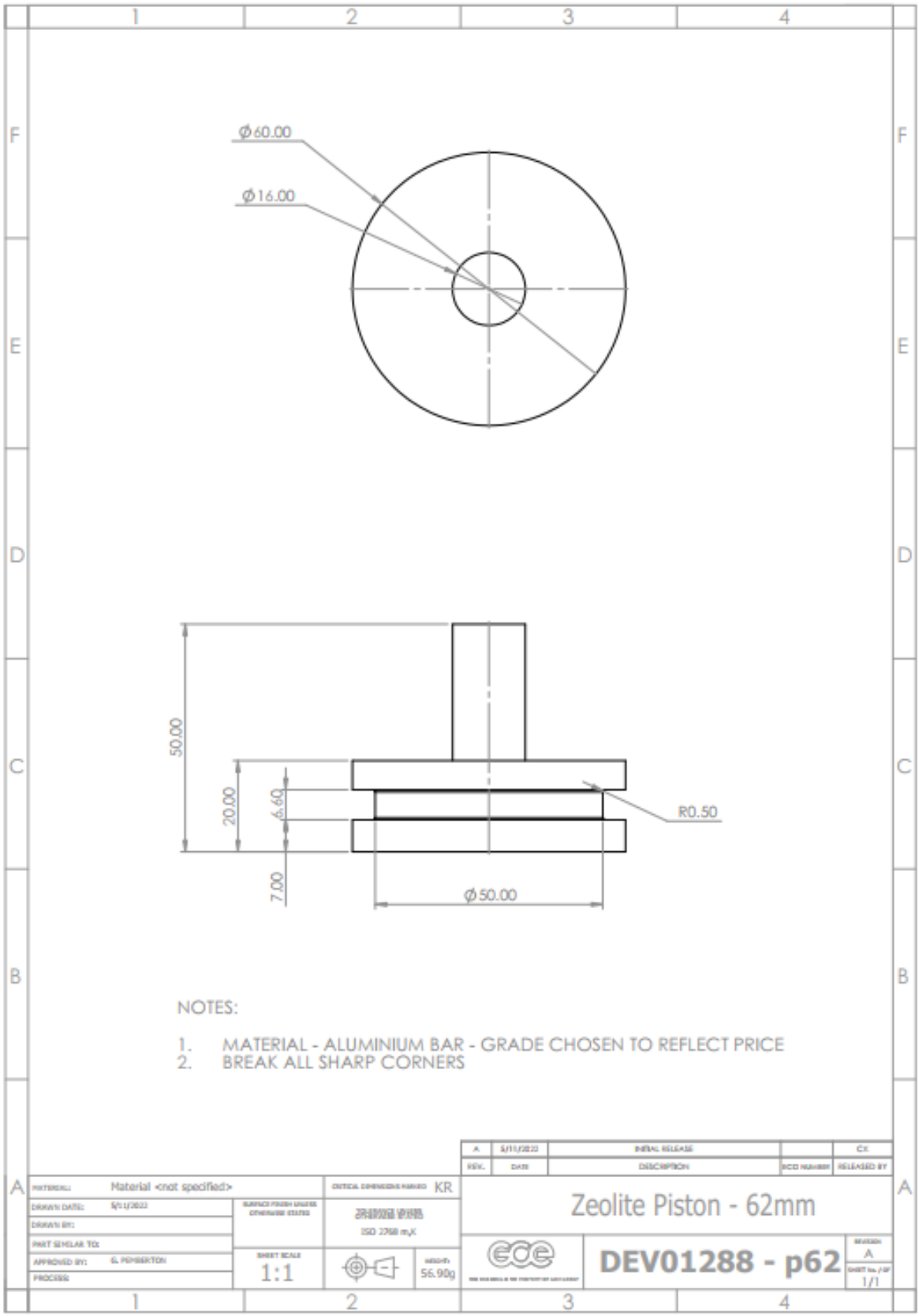

NOTES:

1. MATERIAL - ALUMINIUM BAR - GRADE CHOSEN TO REFLECT PRICE
2. BREAK ALL SHARP CORNERS

REV.	DATE	DESCRIPTION	ECO NUMBER	RELEASED BY
A	5/11/2022	INITIAL RELEASE		CK

MATERIAL:	Material <not specified>
DRAWN DATE:	5/11/2022
DRAWN BY:	
PART SIMILAR TO:	
APPROVED BY:	G. PEMBERTON
PROCESS:	
SURFACE FINISH UNLESS OTHERWISE STATED	
SHEET SCALE	1:1
CRITICAL DIMENSIONS MARKED	KR
ISO 2768 m,K	
WEIGHT	56.90g

Zeolite Piston - 62mm

ece

DEV01288 - p62

REVISION: A

SHEET No. / OF: 1/1